Research Paper

SMARCD3 is a potential prognostic marker and therapeutic target in CAFs

Ming Jiang[1], Huiju Wang[2], Hong Chen[3], Yong Han[2]

[1]Department of General Surgery, People's Hospital of Quzhou, Quzhou, Zhejiang, China
[2]Clinical Research Institute, Zhejiang Provincial People's Hospital, Zhejiang, China. People's Hospital of Hangzhou Medical College, Zhejiang, China. Key Laboratory of Tumor Molecular Diagnosis and Individualized Medicine of Zhejiang Province, Zhejiang, China
[3]Department of Stomatology, Zhejiang Provincial People's Hospital, Hangzhou, China

Correspondence to: Hong Chen, Yong Han; **email:** chenhong@hmc.edu.cn; hanyine@gmail.com, https://orcid.org/0000-0001-9935-2978
Keywords: SMARCD3, colorectal cancer, tumor microenvironment, prognostic marker, therapeutic target
Received: May 13, 2020 **Accepted:** September 5, 2020 **Published:** October 28, 2020

ABSTRACT

Objective: Screening for novel prognostic biomarkers and potential therapeutic targets from colorectal cancer microenvironment.
Results: 372 genes were overexpressed in colorectal cancer microenvironment, five of which that had the most prognostic powers were enriched in Epithelial-Mesenchymal Transition and cell cycle pathways. For the first time, we showed that SMARCD3 was mainly expressed in CAFs and could be a novel prognostic marker and potential therapeutic target. Function analyses indicated that MSARCD3 might promote CAFs activation and colorectal cancer metastasis through SMARCD3-WNT5A/TGF-β-MAPK14-SMARCD3 positive feedback loop. Signaling map of SMARCD3 was constructed and several potential drugs that could regulate SMARCD3 were also presented.
Conclusions: SMARCD3 is a novel prognostic biomarker and potential therapeutic target of colorectal cancer, which may promote cancer metastasis through activation of CAFs.
Methods: Colorectal cancer microenvironment related genes were screened based on immune and stromal scores. Function enrichment analyses were performed to show the underlying mechanistic insights of these tumor microenvironment related genes. Kaplan-Meier survival analysis was used for evaluating the prognostic power. Gene-Pathway interaction network analysis and cellular heterogeneity analysis of tumor microenvironment were also performed. Gene set enrichment analysis was performed for signal gene pathway analysis. Protein data from The Cancer Genome Atlas were used for validation.

INTRODUCTION

Colorectal cancer is one of the most common digestive malignancies worldwide [1]. The tumor microenvironment (TME) plays critical roles in tumorigenesis, development, metastasis and therapeutic responses [2, 3]. For instance, PPM1H (Protein Phosphatase 1H) can inhibit the activation of SMAD signaling pathway and promote mesenchymal differentiation [4]. Knockdown the expression of PPM1H in pancreatic cancer cells can lead to increased expression of vimentin and changes of other epithelial or mesenchymal markers [4–6]. Recently, it is reported that PPM1H knockdown in colorectal cancer cells can induce vimentin expression and activate cancer-associated fibroblasts (CAFs), which in turn can promote the proliferation and migration of colorectal cancer cell with low PPM1H expression [7]. Overexpression and autocrine of WNT2

(Wnt Family Member 2) in CAFs can promote colon cancer proliferation, invasion and metastasis in vitro and in vivo [8, 9]. Exosomes released by CAFs can promote colorectal cancer metastasis and therapeutic resistance by inducing Epithelial-mesenchymal transition (EMT) and tumor cell stemness [10].

Nevertheless, the molecular mechanisms underlying TME associated colorectal cancer progression have never been well elucidated. Hence, screening for novel prognostic biomarkers and potential therapeutic targets for colorectal cancer from TME is of crucial importance. This study takes advantage of publicly available datasets and powerful bioinformatics tools to screen for genes with significant prognostic value and explore potential mechanistic insights.

RESULTS

Screening and function annotation of TME related DEGs in colorectal cancer

Immune score and stromal score of each sample were computed using ESTIMATE algorithm. TME related DEGs were computed based on immune and stromal scores using Agilent microarray expression data and RNAseq data of colon cancer from TCGA. The heat maps of DEGs based on different grouping strategies were presented in Supplementary Figure 1. Supplementary Figure 1A, 1B showed immune and stromal related DEGs computed using Agilent microarray data, while Supplementary Figure 1C, 1D showed DEGs computed using RNAseq data, respectively. Venn diagram analysis indicated that 372 genes were commonly upregulated in immune high and stromal high groups using either Agilent data or RNAseq data (Figure 1A). Details of these 372 genes were presented in Supplementary Table 1.

Gene ontology (GO: biological process, molecular function and cellular component) and KEGG analyses of these 372 genes were performed using network analyst (Figure 1B–1E). Protein-protein interaction (PPI) network was also constructed using network analyst (Figure 1F). As is shown in these figures, immune response, cytokine receptor activity and Toll-like receptor signaling pathway were significantly enriched. Detailed GO, KEGG and PPI results were shown in Supplementary Tables 2–6.

Five genes were associated with poor survival and EMT

Prognostic power of 372 commonly upregulated genes in TME were evaluated through Kaplan-Meier survival analysis using colorectal cancer data from TCGA. Five genes with most significant prognostic power were selected for further analyses. The expression levels of SMARCD3, CRIP2, PRAM1, HSPB2 and CERCAM in Agilent stromal/immune high/low groups and RNAseq stromal/immune high/low groups were demonstrated in Figure 2A. These five genes were all associated with poor OS of patients with colorectal cancer (Figure 2B–2F). Specifically, colorectal cancer patients with SMARCD3 high expression had poorer OS in comparison with patients with SMARCD3 low expression (Hazard ratio: 2.4, logrank p = 0.00031). Similarly, colorectal cancer patients with high expression of CRIP2, PRAM1, HSPB2 or CERCAM had poorer OS comparing with low expressed groups (logrank = 0.0073, 0.0053, 0.0036 and 0.0023, respectively). Moreover, we also built a prognostic model using these five genes. The risk score of each sample was computed based on expression value of the 5 genes using cox proportional hazard model. High risk and low risk groups were divided by the best cutoff point of risk score (Supplementary Figure 2A, upper graph: the distribution of risk scores; lower graph: cutoff point selection based on log rank statistics). Survival analysis results showed that colorectal cancer patients with high risk score had poorer OS comparing with low risk groups (Supplementary Figure 2B, logrank p = 0.0016).

To explore the association among these five genes and different cell types in the tumor microenvironment, cellular heterogeneity analyses of tumor micro-environment were performed using xCell using ssGSEA method. The correlation map of the expression value of five genes and enrichment score of different cell components in TME were shown in Figure 3. As we can see, CRIP2 and PRAM1 are correlated with macrophages while SMARCD3, HSPB2 and CERCAM are associated with fibroblasts (blue represents positive correlation while red represents negative correlation, correlations with p value < 0.05 were presented in the map).

Pathway enrichment analyses of the five genes were performed using GSCAlite. As mentioned in the methods section, pathway activity scores (PAS) of 10 cancer related pathways (such as EMT, apoptosis and cell cycle etc.) in 32 cancer types were computed based on RPPA protein data from TCGA. PAS (gene X^{high}) > PAS (gene X^{low}) indicates gene X has an activation effect, otherwise an inhibition effect. Analyses results indicated that SMARCD3, CRIP2, PRAM1, HSPB2 and CERCAM were associated with epithelial-mesenchymal transition (EMT) pathway activation (upper panel of Figure 4) and cell cycle inhibition (lower panel of Figure 4). Percentage represents ratios of activation or inhibition related cancer types versus 32 cancer types. For instance, SMARCD3 has an activation effect in 6 over 32 cancer types (approximately 19%). Figure 5 shows the gene-pathway interaction map of these five genes in colon cancer. As

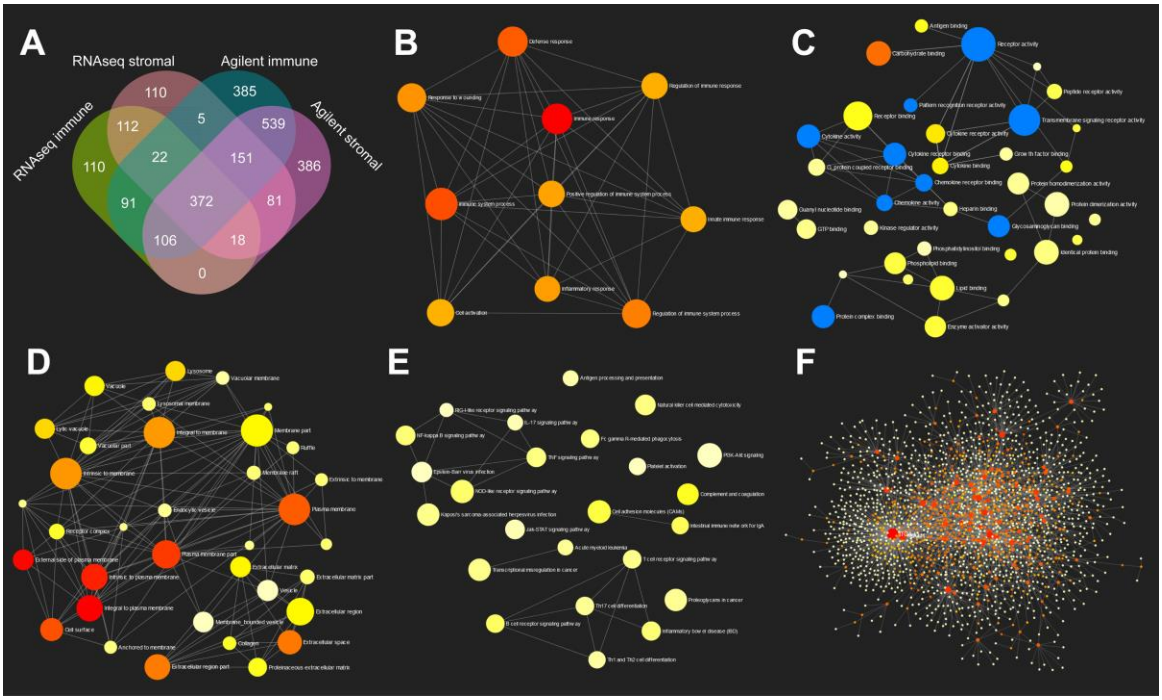

Figure 1. GO and KEGG pathway enrichment network analysis of TME related genes. (**A**) Venn diagram analysis of DEGs based on immune or stromal scores. (**B**–**E**) GO (biological process, molecular function and cellular component) and KEGG pathway enrichment network analysis of 372 commonly upregulated genes in TME. (**F**) Protein-protein interaction network of 372 TME related genes.

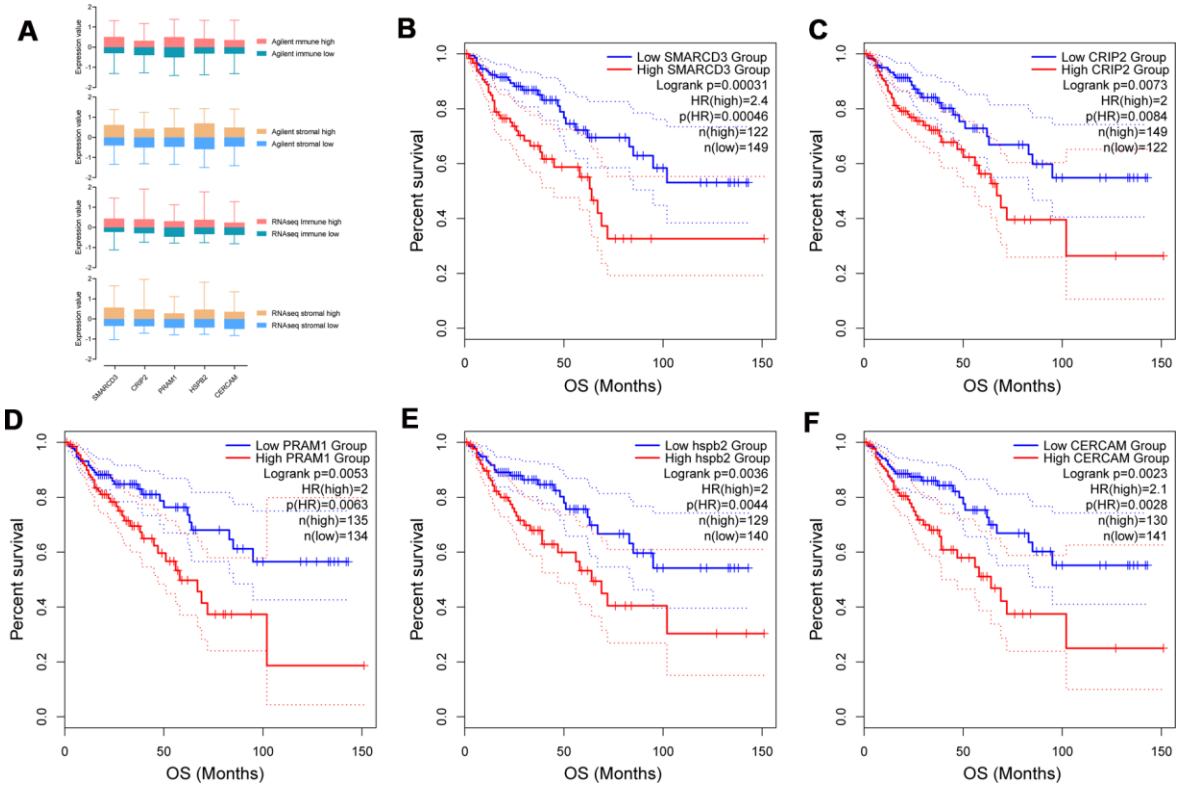

Figure 2. Expression of SMARCD3, CRIP2, PRAM1, HSPB2 and CERCAM in groups with different immune or stromal scores (**A**). Kaplan-Meier survival analysis based on expression value of these genes using TCGA COAD data (**B**–**F**).

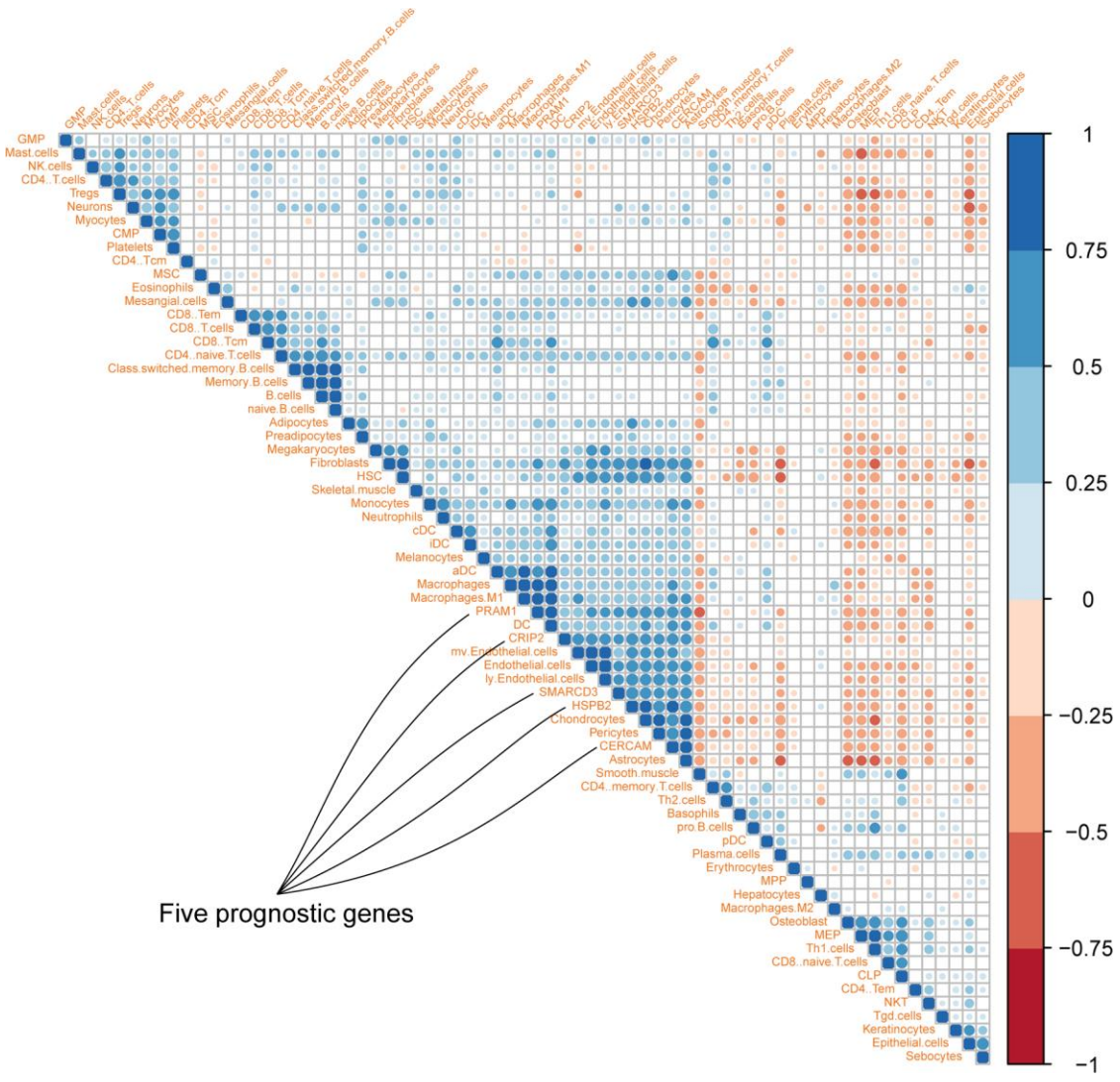

Figure 3. Correlation map of five genes with different cell types in colon cancer microenvironment (Different colors represent spearman r values).

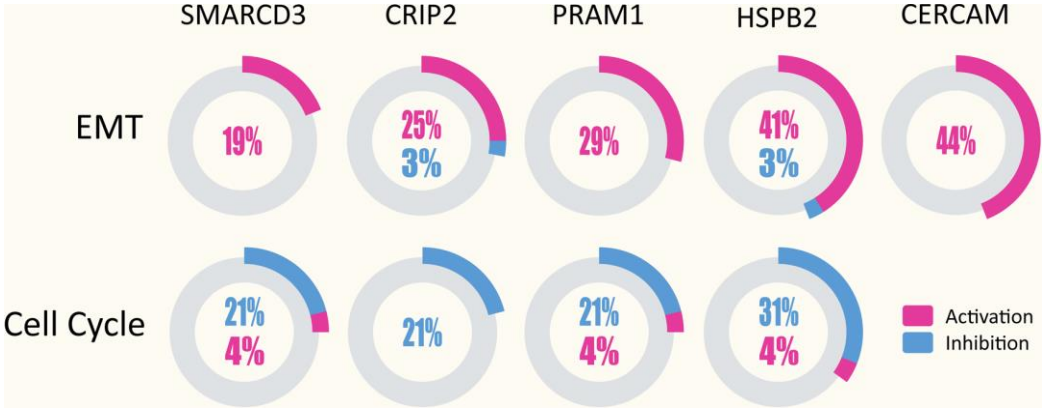

Figure 4. SMARCD3, CRIP2, PRAM1, HSPB2 and CERCAM could activate EMT in multiple cancer types (upper panel), while SMARCD3, CRIP2, PRAM1 and HSPB2 are associated with cell cycle inhibition (lower panel).

we can see, SMARCD3 is associated with cell cycle inhibition and EMT activation, which are in accordance with Figure 4. Moreover, PPI network of these five genes was presented in Supplementary Figure 3.

SMARCD3 expression and function analyses

Based on expression value and literature reports, SMARCD3 were selected for further analysis. Gene expression data analyses based on colon cancer data from TCGA indicated that SMARCD3 is under expressed in cancer tissues comparing with normal control (Supplementary Figure 4A). SMARCD3 expression is higher in stage 3 in comparison with stage 1 (Supplementary Figure 4B). There is no statistical difference of SMARCD3 expression among different gender, body weight, sample type, age groups and TP53 mutation status (Supplementary Figure 4C–4G). Its expression in N2 (positive lymph node between 4 and 9) is higher than in N0 (data not shown). Interestingly, SMARCD3 expression in primary colon tumor is higher than in polyps. Its expression in both polyps and primary tumor is significantly lower than in normal control, which may due to different methylation levels at its promoter region (Supplementary Figure 5). Correlation analyses using SMARCD3 expression data and clinical features of colon cancer patients from TCGA indicated that SMARCD3 expression is associated with lymphatic invasion, OS and copy number etc. (Supplementary Figure 6). The prognostic value of SMARCD3 was further validated using a larger set of TCGA colorectal cancer RNAseq data. As was shown in Supplementary Figure 7, SMARCD3 expression was negatively correlated OS (logrank p = 0.0005, Hazard ratio = 1.867, N = 597), which was consistent with Figure 2B. The prognostic power of SMARCD3 is inferior to the five gene prognostic model presented in Supplementary Figure 2B. IHC data from the protein atlas showed that SMARCD3 were mainly expressed in fibroblasts (Figure 6A). Correlation analysis indicated that SMARCD3 expression was most correlated with fibroblasts (Figure 6B), which was in accordance with Figure 6A.

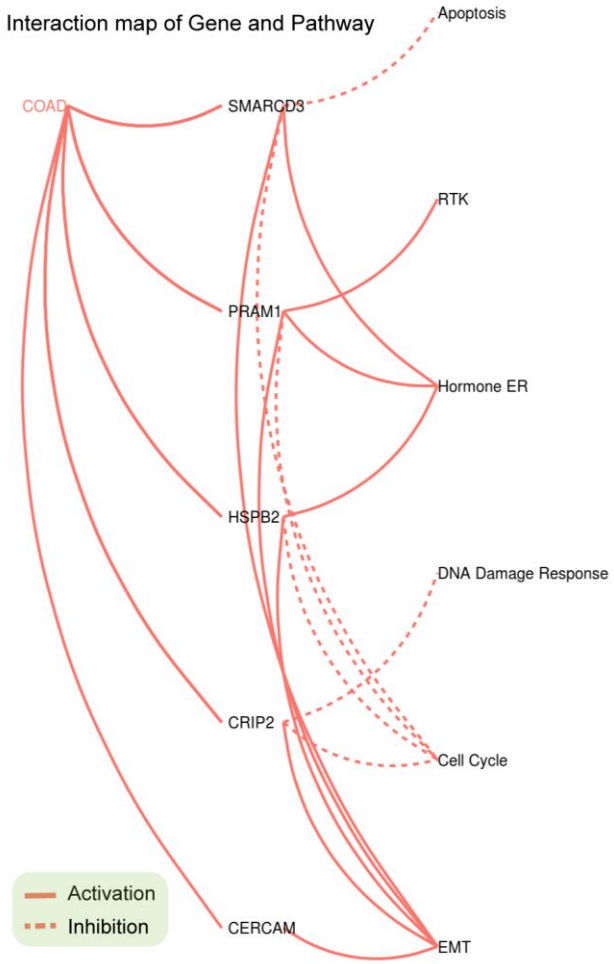

Figure 5. Gene-Pathway interaction network of SMARCD3, CRIP2, PRAM1, HSPB2 and CERCAM in colorectal cancer.

GSEA results showed that SMARCD3 expression was associated with cancer metastasis, TGF-β pathway activation and epithelial-mesenchymal transition (EMT) (Figure 7, $p < 0.0001$, TCGA colorectal cancer RNAseq data, N = 592). Protein level analyses indicated that SMARCD3 expression was negatively correlated with E-Cadherin while positively correlated with N-Cadherin, Fibronectin and SMAD3 (Figure 8, upper graph), which further proved its association with EMT. We also showed that SMARCD3 expression was positively correlated with cell cycle inhibition markers such as p21 an p27, while negatively correlated with cell cycle activation markers such as Cyclin B1 and Cyclin E1 (Figure 8, lower graph). PPI network analysis demonstrated that SMARCD3 could physically interacted with MAPK14 (p38α), MYOD1 and SMAD4 etc. (Supplementary Figure 8), which indicated mechanistic insights underlying SMARCD3 related colorectal cancer metastasis.

Potential molecular mechanisms underlying SMARCD3 associated cancer metastasis

As we mentioned in the above section, SMARCD3 was associated with cancer metastasis and EMT related gene signatures. Further PPI analysis indicated that SMARCD3 might promote colorectal cancer metastasis through MAPK14, MYOD1 or SMAD4 related pathways. Previously, it was reported that SMARCD3 could stimulate EMT of breast cancer cells through

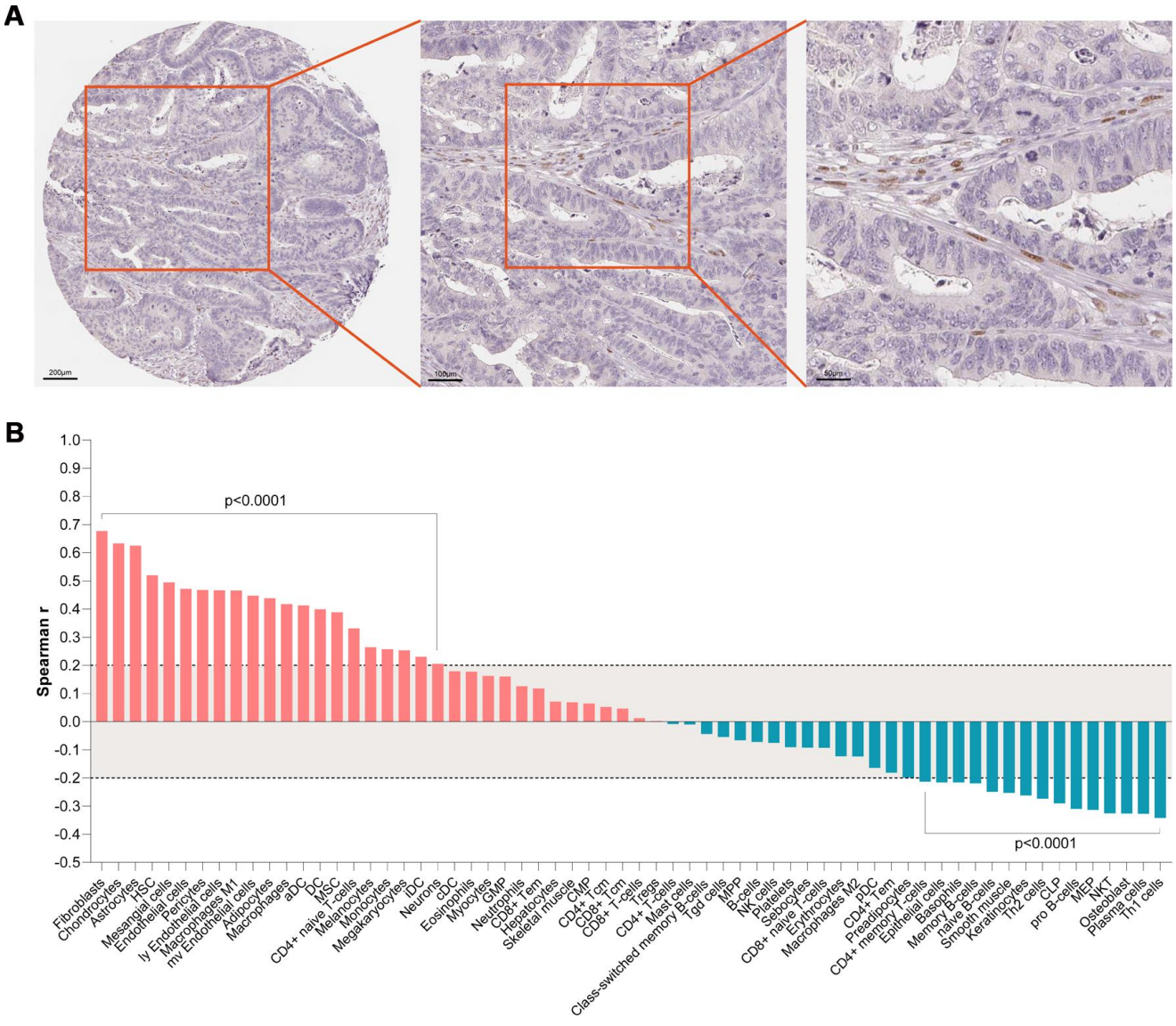

Figure 6. (**A**) IHC staining indicated that SMARCD3 was mainly expressed colon cancer associated fibroblasts. (**B**) SMARCD3 expression was most associated with fibroblasts by ssGSEA analysis.

upregulating WNT5A expression [11]. While Wnt5a and Wnt11 could regulate EMT by inducing p38 (Mapk14) phosphorylation in mouse early development [12]. Hence, we can speculate that SMARCD3 could potentially promote EMT through WNT5A-MAPK14 pathway. Moreover, it was reported that MAPK14 could induce SMARCD3 phosphorylation and promote the incorporation of MYOD1-SMARCD3 into a Brg1-based SWI/SNF complex. This complex could activate the transcription activity of MYOD1 [13] and led to upregulation of EMT related genes such as Vimentin and SNAIL [14]. These reports indicated that MAPK14 could regulate EMT by phosphorylating SMARCD3. So, we can conclude that there is a positive feedback loop among SMARCD3, WNT5A and MAPK14. Moreover, it was reported that TGF-β could also promote EMT through MAPK14 phosphorylation [15], which indicated its involvement in the process of SMARCD3 promoted EMT.

Using TCGA colorectal cancer RNAseq and protein expression data, we demonstrated that WNT5A (Supplementary Figure 9A) and TGFB1 (Supplementary Figure 9C) were positively correlated with SMARCD3; WNT5A (Supplementary Figure 9B) and TGFB1 (Supplementary Figure 9D) were overexpressed in SMARCD3 high group. We also showed that SMARCD3 was associated with MAPK14 phosphorylation level (Supplementary Figure 10). The above results were consistent with the above literature reports and our speculations. Based on the above results, we could summarize two potential positive feedback loops: SMARCD3-WNT5A-MAPK14-SMARCD3 and SMARCD3-TGF-β-MAPK14-SMARCD3 (Figure 9). Besides, data mining using multiple gene-drug datasets such as CTDbase and GSCAlite were performed in this study. We proposed several drugs that could target SMARCD3, which were presented in Figure 9.

DISCUSSION

In this study, we found 372 genes that overexpressed in TME based on immune score and stromal score using TCGA COAD data from two platforms (Agilent and RNAseq). GO and KEGG pathway enrichment analyses showed that these 372 genes were enriched in immune response, cytokine production and toll-like receptor signaling pathway etc. SMARCD3, CRIP2, PRAM1, HSPB2 and CERCAM were selected for further analyses due to their most significant prognostic powers. Cellular heterogeneity analysis indicated that PRAM1 was associated with macrophages while SMARCD3, CRIP2,

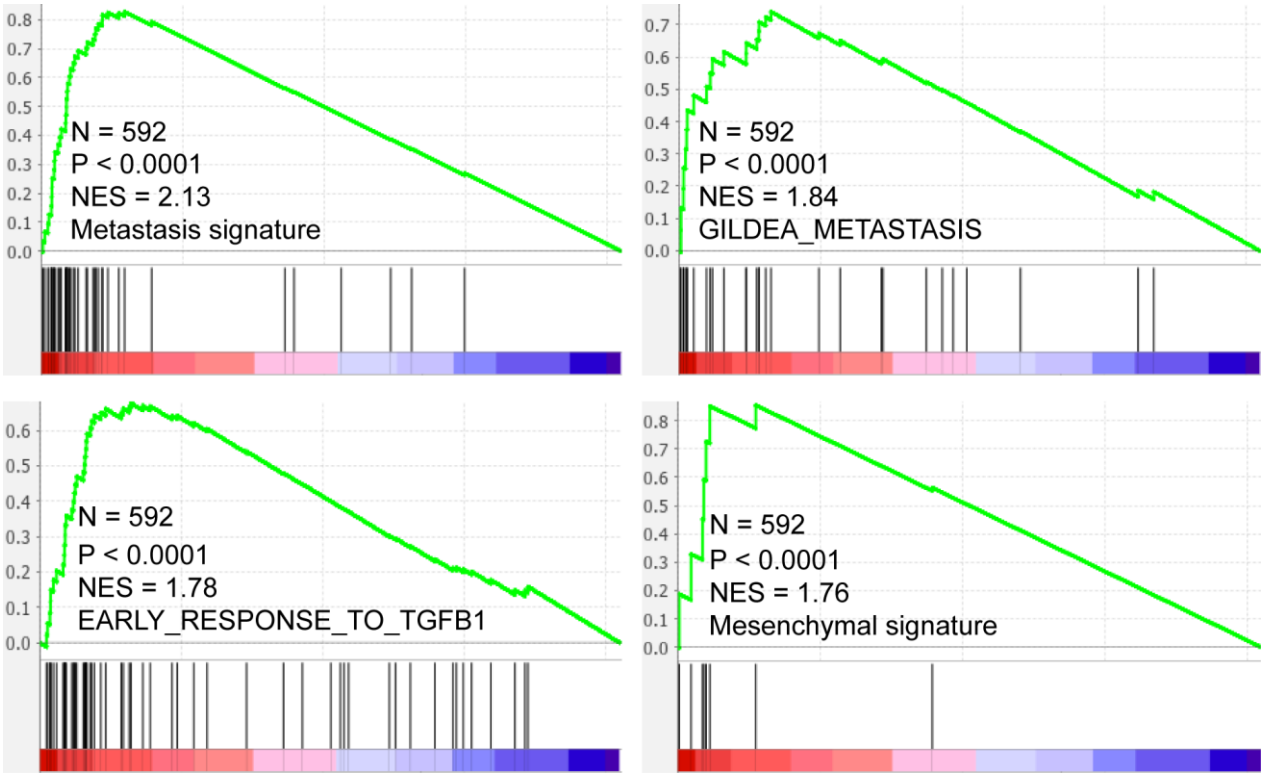

Figure 7. SMARCD3 expression is positively correlated with metastasis, TGF-β pathway activation and Mesenchymal signatures.

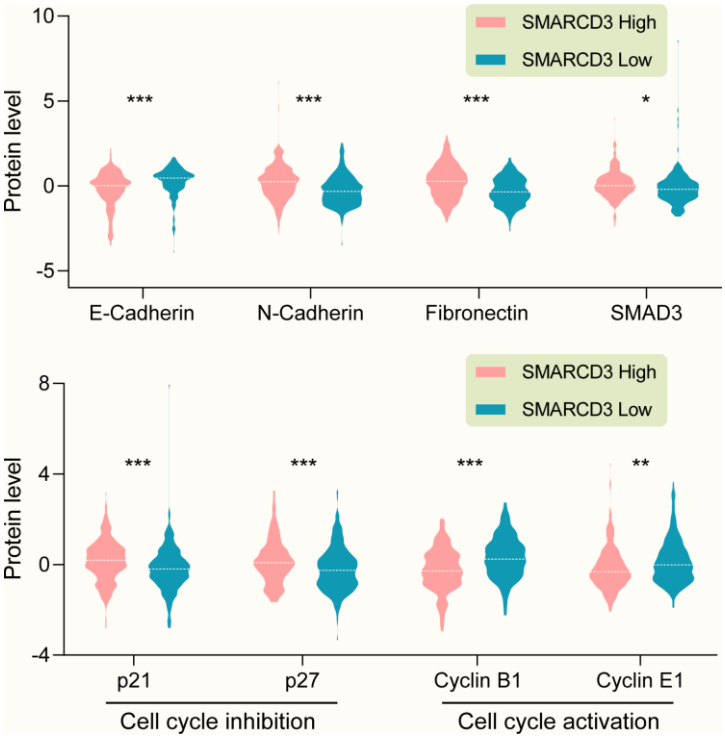

Figure 8. (Upper graph) SMARCD3 expression is negatively correlated with E-Cadherin, while positively correlated with N-Cadherin, Fibronectin and SMAD3. (Lower graph) SMARCD3 expression is positively correlated with cell cycle inhibitor p21 and p27, while negatively correlated with cell cycle activator Cyclin B1 and Cyclin E1.

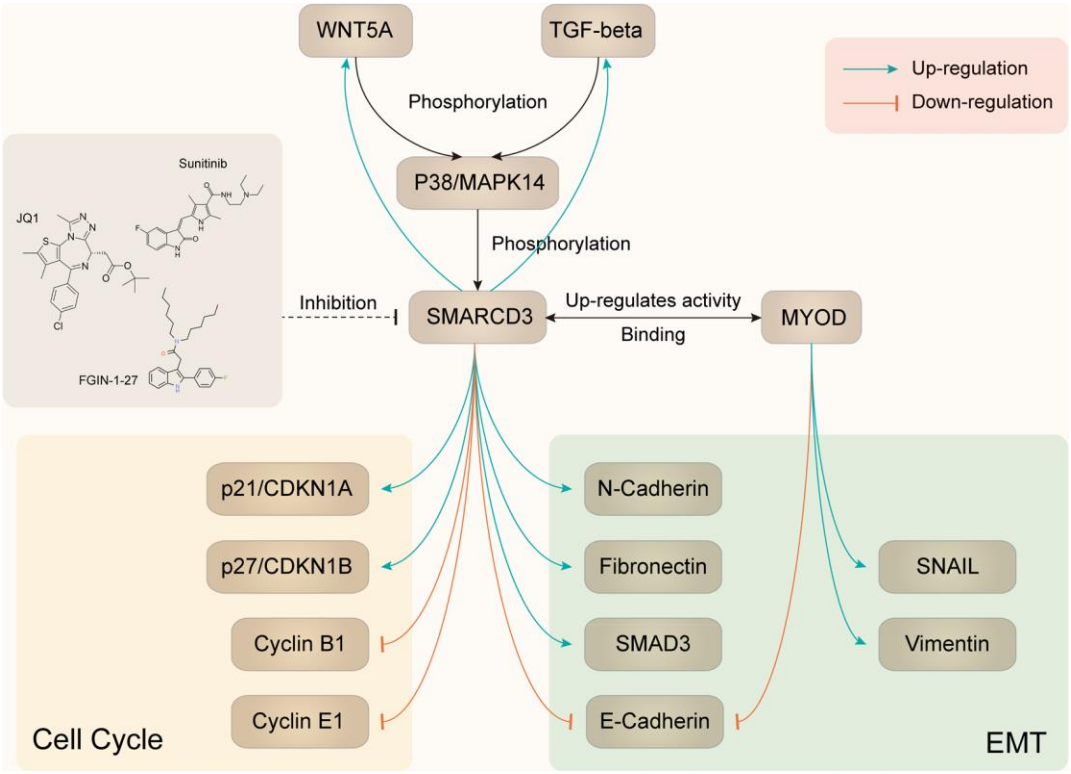

Figure 9. Summary of SMARCD3 interaction network.

HSPB2 and CERCAM were correlated with fibroblasts. Pathway analyses showed that the five genes were involved in EMT activation and cell cycle inhibition. Since EMT was an important factor for CAFs activation, the above results implicated a potential role of these genes in inducing CAFs activation.

CAFs plays critical roles in tumor proliferation, invasion, angiogenesis and regulation of tumor immune microenvironment. For instance, CAFs could release exosomes, VEGF (vascular endothelial growth factor), HGF (hepatocyte growth factor) and GAS6 (growth arrest-specific gene 6) to promote cancer proliferation and invasion, and affect the function of epithelial cell and macrophages [16]; regulate cancer metastasis, therapeutic responses and T cell function through matrix remodeling including matrix production, proteolysis and matrix crosslinking [17, 18]; promote cancer cell growth through metabolic effects such as lactate shuttling, amino acid depletion and alanine aspartate shuttling [19, 20]; and regulate cancer immune microenvironment through TGF-β, IL-6, CXCL12 (CXC- chemokine ligand 12) and CCL2 (CC-chemokine ligand 2) [21–23].

SMARCD3 (SWI/SNF Related, Matrix Associated, Actin Dependent Regulator of Chromatin, Subfamily D, Member 3) encoded protein belongs to SWI/SNF family which display helicase and ATPase activities and could regulate gene transcription by altering the chromatin. It was reported that knock down SMARCD3 expression could induce mesenchymal-epithelial transition (EMT) of breast cancer cells [24]. Here, we showed that SMARCD3 was mainly expressed in fibroblasts and was associated with EMT and tumor metastasis. Its expression was positively correlated with mesenchymal biomarkers such as N-Cadherin and Fibronectin while negatively correlated with epithelial biomarkers like E-Cadherin. Literature mining indicated that SMARCD3 could upregulate WNT5A and TGF-β expression, which could induce MAPK14 phosphorylation. Then the phosphorylated MAPK14 could further induce SMARCD3 phosphorylation and promote the incorporation of MYOD1-SMARCD3 into a Brg1-based SWI/SNF complex and finally led to EMT. Using colorectal cancer data, we showed that SMARCD3 expression was positively correlated with WNT5A, TGF-β and p-MAPK14, which were consistent with previous reports.

Based on the above findings, we speculated that SMARCD3-WNT5A/TGF-β-MAPK14-SMARCD3 positive feedback loop might be activated in fibroblasts and play critical roles in promoting CAFs activation and cancer metastasis (as detailed in Figure 9).

In summary, we reported 372 colorectal cancer TME related genes, five of them that have the most prognostic powers were enriched in EMT and cell cycle pathways. For the first time, we demonstrated that SMARCD3 was a novel prognostic marker that mainly expressed in CAFs and might promote CAFs activation and colorectal cancer metastasis through SMARCD3-WNT5A/TGF-β-MAPK14-SMARCD3 positive feedback loop. Hence, screening for drugs or chemicals targeting SMARCD3 may exert important clinical impact on colorectal cancer management.

MATERIALS AND METHODS

Ethics statement

All the data used in this study were downloaded from publicly available sources. The Research Ethics Committee of Zhejiang Provincial people's Hospital waived the requirement for ethical approval.

Data source

Agilent microarray and RNAseq expression data were downloaded from The Cancer Genome Atlas (TCGA: http://cancergenome.nih.gov/). Expression profiles of colon, polyp and primary colon cancer were obtained from Gene Expression Omnibus (GEO, accession no.GSE41258) [25, 26]. IHC staining results of SMARCD3 (https://images.proteinatlas.org/63955/147563_A_2_8.jpg), Protein expression and phosphorylation data were obtained from Protein atlas [27] (https://www.proteinatlas.org) and TCGA. Chemical-gene interaction and protein-protein interaction data was downloaded from The Comparative Toxicogenomics Database (CTD base) [28] and GSCAlite [29].

Bioinformatics and statistical analyses

The immune score and stromal score of each colon cancer samples were computed based on ESTIMATE algorithm using RNAseq data from TCGA [30]. Heat map and clustering analyses were performed using MeV software (http://mev.tm4.org). Gene Set Enrichment analysis (GSEA) was performed to show the functional enrichment of SMARCD3 in breast cancer using GSEA v4.0.3 (https://www.gsea-msigdb.org/gsea/downloads.jsp). Protein-protein interaction network was visualized through GeneMANIA plugin [31] in the Cytoscape environment [32]. Venn diagram was drawn using an online tool (http://bioinformatics.psb.ugent.be/webtools/Venn/). GO and KEGG pathway enrichment analyses and visualization were performed using NetworkAnalyst [33]. Survival analysis module of GEPIA2 web tool and Graphpad Prism 8 (2365

Northside Dr., Suite 560, San Diego, CA 92108, USA) was used for Kaplan-Meier analyses [34].

Gene-pathway interaction network analysis was performed using GSCAlite [29]. Briefly, pathway activity groups (activation and inhibition) is defined by pathway scores computed based on RPPA protein data from TCGA, 10 pathways and 32 cancer types are included. Gene expression positively correlated with pathway activity score are considered to have an activate effect to a pathway, otherwise have an inhibit effect to a pathway. Cellular heterogeneity analyses of tumor microenvironment were performed using xCell using ssGSEA method [35]. Correlation map was drew using corrPlot package [36] in R 3.6.3 (R Foundation for Statistical Computing [http://www.r-project.org/]). Expression of SMARCD3 in different clinical groups and its correlation with methylation were plotted using UALCAN based on data from TCGA [37]. The heat map of SMARCD3 expression and clinical features such as tumor stage, lymphatic invasion and overall survival was plotted using MEXPRESS online tool [38].

Risk score of each sample was computed based on expression value of the 5 genes using cox proportional hazard model. The best cutoff value of 5 gene risk score was computed using survminer package (https://rpkgs.datanovia.com/survminer/index.html) and Kaplan-Meier analyses were performed through survival package [39] in R. All other statistical analyses were perform using R or GraphPad Prism 8. Standard statistical tests including paired t-test, fisher exact test and independent samples t-test were employed in the data analyses. Adjust P value was corrected for multiple comparisons using the Benjamini and Hochberg's false discovery rate [40]. Significance was defined as a P value < 0.05.

Availability of data

Data sharing is not applicable to this article as no new data were created or analyzed in this study.

AUTHOR CONTRIBUTIONS

Conceived and designed the experiments: Ming Jiang, Hong Chen, Yong Han. Performed the experiments: Ming Jiang, Huiju Wang, Hong Chen, Yong Han. Analyzed the data: Ming Jiang, Hong Chen, Yong Han. Wrote the paper: Ming Jiang, Huiju Wang, Hong Chen, Yong Han.

CONFLICTS OF INTEREST

The authors declare that they have no conflicts of interest.

FUNDING

National Natural Science Foundation of China, Grant Number: 81702774. Natural Science Foundation of Zhejiang Province, No. LY17H160065 Zhejiang Provincial Administration of Traditional Chinese Medicine, Grant Number: 2016ZB018. Zhejiang Provincial Medical and Healthy Science and Technology Projects (Grant No. 2020KY449 and 2018KY016).

REFERENCES

1. Torre LA, Bray F, Siegel RL, Ferlay J, Lortet-Tieulent J, Jemal A. Global cancer statistics, 2012. CA Cancer J Clin. 2015; 65:87–108. https://doi.org/10.3322/caac.21262 PMID:25651787

2. Maman S, Witz IP. A history of exploring cancer in context. Nat Rev Cancer. 2018; 18:359–76. https://doi.org/10.1038/s41568-018-0006-7 PMID:29700396

3. Lu Z, Peng Z, Liu C, Wang Z, Wang Y, Jiao X, Li J, Shen L. Current status and future perspective of immunotherapy in gastrointestinal cancers. The Innovation. 2020; 1.w https://doi.org/10.1016/j.xinn.2020.100041

4. Shen T, Sun C, Zhang Z, Xu N, Duan X, Feng XH, Lin X. Specific control of BMP signaling and mesenchymal differentiation by cytoplasmic phosphatase PPM1H. Cell Res. 2014; 24:727–41. https://doi.org/10.1038/cr.2014.48 PMID:24732009

5. Zhu H, Qin H, Li DM, Liu J, Zhao Q. Effect of PPM1H on Malignant phenotype of human pancreatic cancer cells. Oncol Rep. 2016; 36:2926–34. https://doi.org/10.3892/or.2016.5065 PMID:27599670

6. Lee-Hoeflich ST, Pham TQ, Dowbenko D, Munroe X, Lee J, Li L, Zhou W, Haverty PM, Pujara K, Stinson J, Chan SM, Eastham-Anderson J, Pandita A, et al. PPM1H is a p27 phosphatase implicated in trastuzumab resistance. Cancer Discov. 2011; 1:326–37. https://doi.org/10.1158/2159-8290.CD-11-0062 PMID:22586611

7. Xu X, Zhu L, Yang Y, Pan Y, Feng Z, Li Y, Chang W, Sui J, Cao F. Low tumour PPM1H indicates poor prognosis in colorectal cancer via activation of cancer-associated fibroblasts. Br J Cancer. 2019; 120:987–95. https://doi.org/10.1038/s41416-019-0450-5 PMID:30988394

8. Kramer N, Schmöllerl J, Unger C, Nivarthi H, Rudisch A, Unterleuthner D, Scherzer M, Riedl A, Artaker M, Crncec I, Lenhardt D, Schwarz T, Prieler B, et al. Autocrine WNT2 signaling in fibroblasts promotes

colorectal cancer progression. Oncogene. 2017; 36:5460–72.
https://doi.org/10.1038/onc.2017.144 PMID:28553956

9. Unterleuthner D, Neuhold P, Schwarz K, Janker L, Neuditschko B, Nivarthi H, Crncec I, Kramer N, Unger C, Hengstschläger M, Eferl R, Moriggl R, Sommergruber W, et al. Cancer-associated fibroblast-derived WNT2 increases tumor angiogenesis in colon cancer. Angiogenesis. 2020; 23:159–77.
https://doi.org/10.1007/s10456-019-09688-8
PMID:31667643

10. Hu JL, Wang W, Lan XL, Zeng ZC, Liang YS, Yan YR, Song FY, Wang FF, Zhu XH, Liao WJ, Liao WT, Ding YQ, Liang L. CAFs secreted exosomes promote metastasis and chemotherapy resistance by enhancing cell stemness and epithelial-mesenchymal transition in colorectal cancer. Mol Cancer. 2019; 18:91.
https://doi.org/10.1186/s12943-019-1019-x
PMID:31064356

11. Jordan NV, Prat A, Abell AN, Zawistowski JS, Sciaky N, Karginova OA, Zhou B, Golitz BT, Perou CM, Johnson GL. SWI/SNF chromatin-remodeling factor Smarcd3/Baf60c controls epithelial-mesenchymal transition by inducing Wnt5a signaling. Mol Cell Biol. 2013; 33:3011–25.
https://doi.org/10.1128/MCB.01443-12
PMID:23716599

12. Andre P, Song H, Kim W, Kispert A, Yang Y. Wnt5a and Wnt11 regulate mammalian anterior-posterior axis elongation. Development. 2015; 142:1516–27.
https://doi.org/10.1242/dev.119065 PMID:25813538

13. Forcales SV, Albini S, Giordani L, Malecova B, Cignolo L, Chernov A, Coutinho P, Saccone V, Consalvi S, Williams R, Wang K, Wu Z, Baranovskaya S, et al. Signal-dependent incorporation of MyoD-BAF60c into Brg1-based SWI/SNF chromatin-remodelling complex. EMBO J. 2012; 31:301–16.
https://doi.org/10.1038/emboj.2011.391
PMID:22068056

14. de la Serna IL, Ohkawa Y, Berkes CA, Bergstrom DA, Dacwag CS, Tapscott SJ, Imbalzano AN. MyoD targets chromatin remodeling complexes to the myogenin locus prior to forming a stable DNA-bound complex. Mol Cell Biol. 2005; 25:3997–4009.
https://doi.org/10.1128/MCB.25.10.3997-4009.2005
PMID:15870273

15. Hedrick E, Safe S. Transforming growth factor β/NR4A1-inducible breast cancer cell migration and epithelial-to-mesenchymal transition is p38α (mitogen-activated protein kinase 14) dependent. Mol Cell Biol. 2017; 37:e00306–17.
https://doi.org/10.1128/MCB.00306-17
PMID:28674186

16. Sahai E, Astsaturov I, Cukierman E, DeNardo DG, Egeblad M, Evans RM, Fearon D, Greten FR, Hingorani SR, Hunter T, Hynes RO, Jain RK, Janowitz T, et al. A framework for advancing our understanding of cancer-associated fibroblasts. Nat Rev Cancer. 2020; 20:174–86.
https://doi.org/10.1038/s41568-019-0238-1
PMID:31980749

17. Kechagia JZ, Ivaska J, Roca-Cusachs P. Integrins as biomechanical sensors of the microenvironment. Nat Rev Mol Cell Biol. 2019; 20:457–73.
https://doi.org/10.1038/s41580-019-0134-2
PMID:31182865

18. Zeltz C, Primac I, Erusappan P, Alam J, Noel A, Gullberg D. Cancer-associated fibroblasts in desmoplastic tumors: emerging role of integrins. Semin Cancer Biol. 2020; 62:166–81.
https://doi.org/10.1016/j.semcancer.2019.08.004
PMID:31415910

19. Sanford-Crane H, Abrego J, Sherman MH. Fibroblasts as modulators of local and systemic cancer metabolism. Cancers (Basel). 2019; 11:619.
https://doi.org/10.3390/cancers11050619
PMID:31058816

20. Bertero T, Oldham WM, Grasset EM, Bourget I, Boulter E, Pisano S, Hofman P, Bellvert F, Meneguzzi G, Bulavin DV, Estrach S, Feral CC, Chan SY, et al. Tumor-stroma mechanics coordinate amino acid availability to sustain tumor growth and Malignancy. Cell Metab. 2019; 29:124–40.e10.
https://doi.org/10.1016/j.cmet.2018.09.012
PMID:30293773

21. Chakravarthy A, Khan L, Bensler NP, Bose P, De Carvalho DD. TGF-β-associated extracellular matrix genes link cancer-associated fibroblasts to immune evasion and immunotherapy failure. Nat Commun. 2018; 9:4692.
https://doi.org/10.1038/s41467-018-06654-8
PMID:30410077

22. Chen IX, Chauhan VP, Posada J, Ng MR, Wu MW, Adstamongkonkul P, Huang P, Lindeman N, Langer R, Jain RK. Blocking CXCR4 alleviates desmoplasia, increases T-lymphocyte infiltration, and improves immunotherapy in metastatic breast cancer. Proc Natl Acad Sci USA. 2019; 116:4558–66.
https://doi.org/10.1073/pnas.1815515116
PMID:30700545

23. Fearon DT. The carcinoma-associated fibroblast expressing fibroblast activation protein and escape from immune surveillance. Cancer Immunol Res. 2014; 2:187–93.
https://doi.org/10.1158/2326-6066.CIR-14-0002
PMID:24778314

24. Gregoire JM, Fleury L, Salazar-Cardozo C, Alby F, Masson V, Arimondo PB, Ausseil F. Identification of epigenetic factors regulating the mesenchyme to epithelium transition by RNA interference screening in breast cancer cells. BMC Cancer. 2016; 16:700. https://doi.org/10.1186/s12885-016-2683-5 PMID:27581651

25. Martin ML, Zeng Z, Adileh M, Jacobo A, Li C, Vakiani E, Hua G, Zhang L, Haimovitz-Friedman A, Fuks Z, Kolesnick R, Paty PB. Logarithmic expansion of LGR5^{+} cells in human colorectal cancer. Cell Signal. 2018; 42:97–105. https://doi.org/10.1016/j.cellsig.2017.09.018 PMID:28958617

26. Barrett T, Wilhite SE, Ledoux P, Evangelista C, Kim IF, Tomashevsky M, Marshall KA, Phillippy KH, Sherman PM, Holko M, Yefanov A, Lee H, Zhang N, et al. NCBI GEO: archive for functional genomics data sets--update. Nucleic Acids Res. 2013; 41:D991–5. https://doi.org/10.1093/nar/gks1193 PMID:23193258

27. Uhlen M, Zhang C, Lee S, Sjöstedt E, Fagerberg L, Bidkhori G, Benfeitas R, Arif M, Liu Z, Edfors F, Sanli K, von Feilitzen K, Oksvold P, et al. A pathology atlas of the human cancer transcriptome. Science. 2017; 357:eaan2507. https://doi.org/10.1126/science.aan2507 PMID:28818916

28. Davis AP, Grondin CJ, Johnson RJ, Sciaky D, McMorran R, Wiegers J, Wiegers TC, Mattingly CJ. The comparative toxicogenomics database: update 2019. Nucleic Acids Res. 2019; 47:D948–54. https://doi.org/10.1093/nar/gky868 PMID:30247620

29. Liu CJ, Hu FF, Xia MX, Han L, Zhang Q, Guo AY. GSCALite: a web server for gene set cancer analysis. Bioinformatics. 2018; 34:3771–72. https://doi.org/10.1093/bioinformatics/bty411 PMID:29790900

30. Yoshihara K, Shahmoradgoli M, Martínez E, Vegesna R, Kim H, Torres-Garcia W, Treviño V, Shen H, Laird PW, Levine DA, Carter SL, Getz G, Stemke-Hale K, et al. Inferring tumour purity and stromal and immune cell admixture from expression data. Nat Commun. 2013; 4:2612. https://doi.org/10.1038/ncomms3612 PMID:24113773

31. Montojo J, Zuberi K, Rodriguez H, Kazi F, Wright G, Donaldson SL, Morris Q, Bader GD. GeneMANIA cytoscape plugin: fast gene function predictions on the desktop. Bioinformatics. 2010; 26:2927–28. https://doi.org/10.1093/bioinformatics/btq562 PMID:20926419

32. Shannon P, Markiel A, Ozier O, Baliga NS, Wang JT, Ramage D, Amin N, Schwikowski B, Ideker T. Cytoscape: a software environment for integrated models of biomolecular interaction networks. Genome Res. 2003; 13:2498–504. https://doi.org/10.1101/gr.1239303 PMID:14597658

33. Zhou G, Soufan O, Ewald J, Hancock RE, Basu N, Xia J. NetworkAnalyst 3.0: a visual analytics platform for comprehensive gene expression profiling and meta-analysis. Nucleic Acids Res. 2019; 47:W234–41. https://doi.org/10.1093/nar/gkz240 PMID:30931480

34. Tang Z, Kang B, Li C, Chen T, Zhang Z. GEPIA2: an enhanced web server for large-scale expression profiling and interactive analysis. Nucleic Acids Res. 2019; 47:W556–60. https://doi.org/10.1093/nar/gkz430 PMID:31114875

35. Aran D, Hu Z, Butte AJ. xCell: digitally portraying the tissue cellular heterogeneity landscape. Genome Biol. 2017; 18:220. https://doi.org/10.1186/s13059-017-1349-1 PMID:29141660

36. Taiyun Wei VS. R package "corrplot": Visualization of a Correlation Matrix (Version 0.84). 2017.

37. Chandrashekar DS, Bashel B, Balasubramanya SA, Creighton CJ, Ponce-Rodriguez I, Chakravarthi BV, Varambally S. UALCAN: a portal for facilitating tumor subgroup gene expression and survival analyses. Neoplasia. 2017; 19:649–58. https://doi.org/10.1016/j.neo.2017.05.002 PMID:28732212

38. Koch A, Jeschke J, Van Criekinge W, van Engeland M, De Meyer T. MEXPRESS update 2019. Nucleic Acids Res. 2019; 47:W561–65. https://doi.org/10.1093/nar/gkz445 PMID:31114869

39. Therneau TM. A Package for Survival Analysis in R. R package version 32–3. 2020.

40. Benjamini Y, Hochberg Y. Controlling the false discovery rate: a practical and powerful approach to multiple testing. Journal of the Royal Statistical Society Series B (Methodological). 1995; 57:289–300. https://doi.org/10.1111/j.2517-6161.1995.tb02031.x

SUPPLEMENTARY MATERIALS

Supplementary Figures

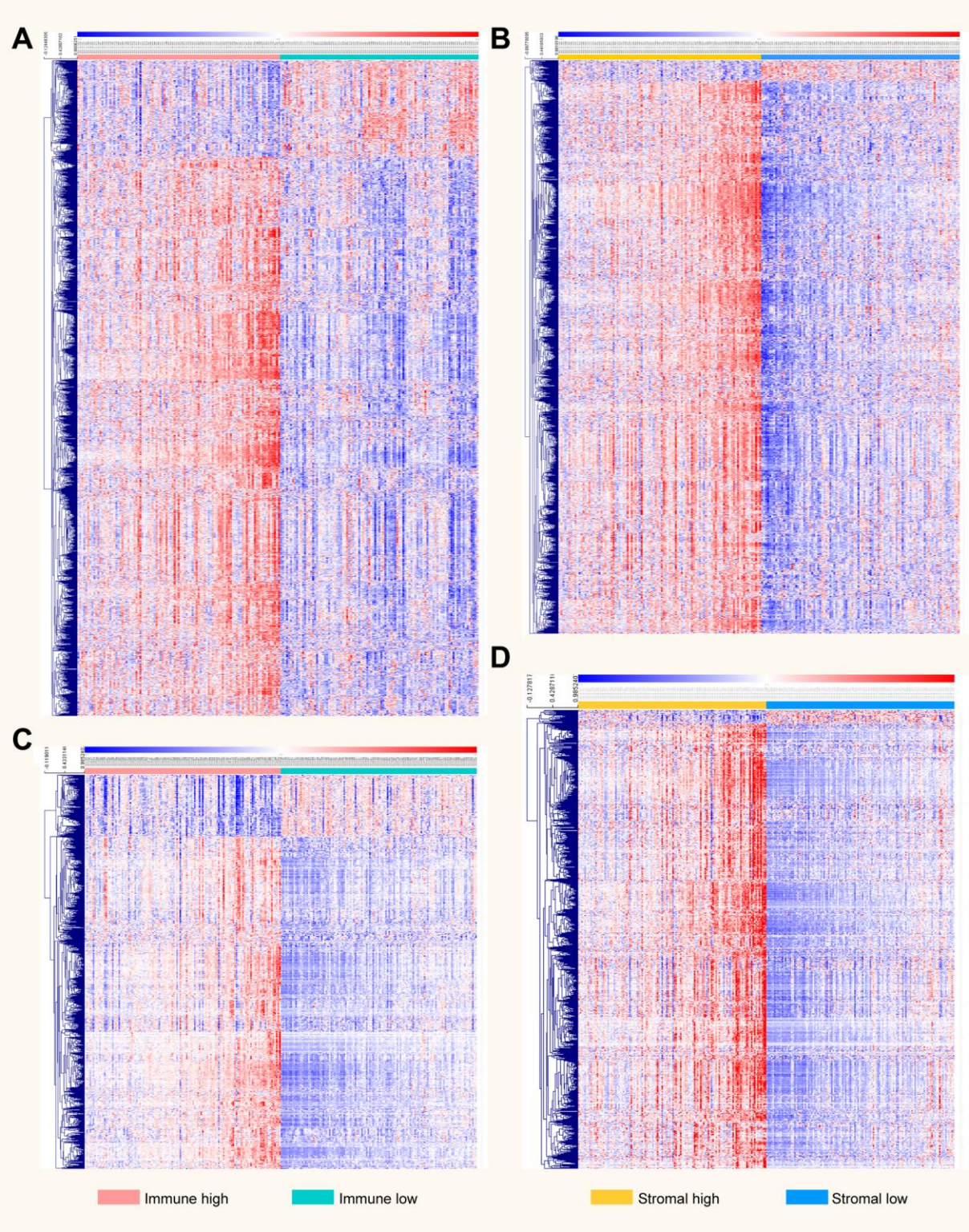

Supplementary Figure 1. Heat map of TME related genes. DEGs computed based on immune (**A**) or stromal score (**B**) using HNSC Agilent microarray data. DEGs computed based on immune (**C**) or stromal score (**D**) using HNSC RNAseq data.

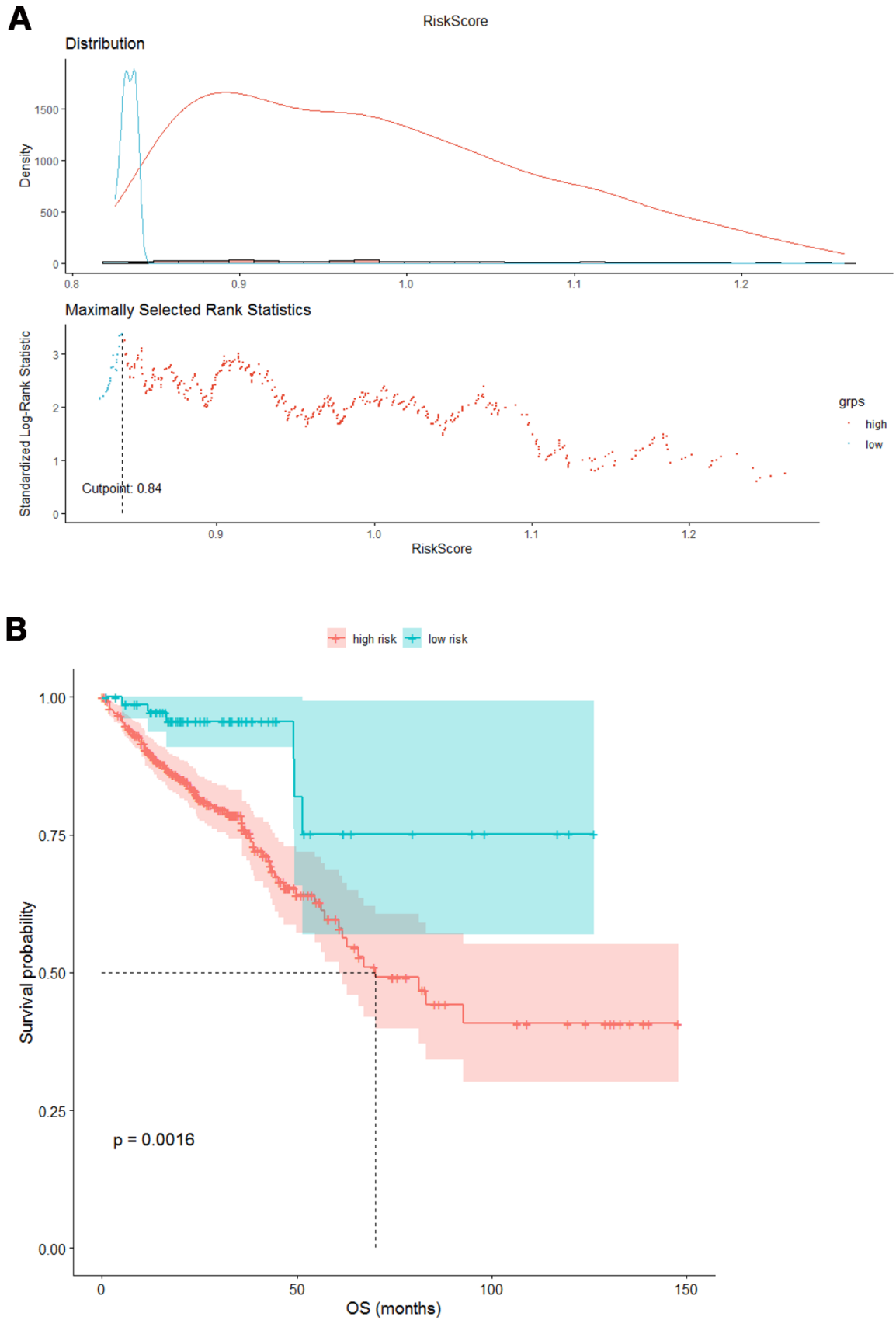

Supplementary Figure 2. (**A**) Upper graph: the distribution of risk scores; lower graph: cutoff point selection based on log rank statistics. (**B**) Kaplan-Meier survival analysis of high risk and low risk groups.

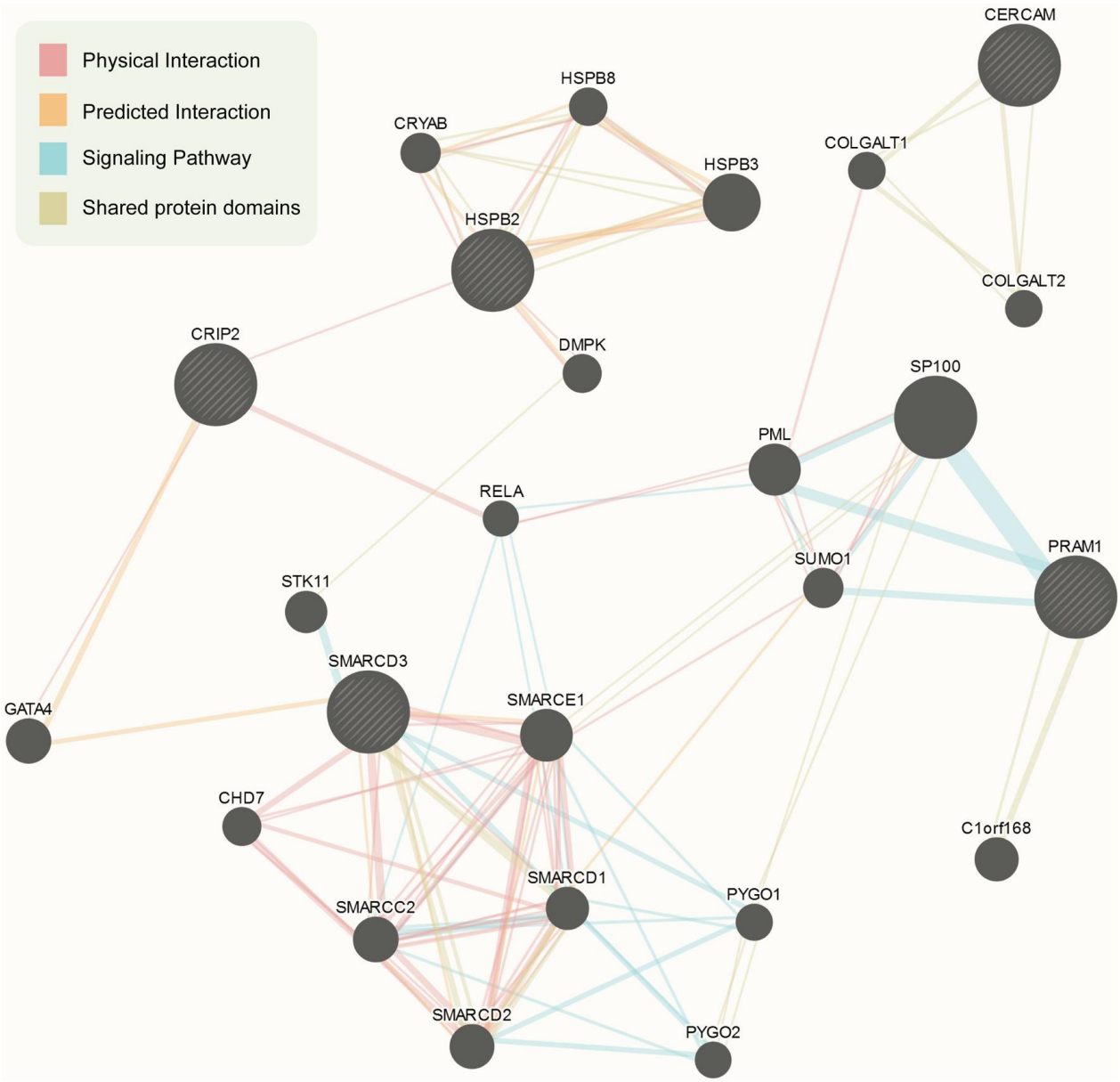

Supplementary Figure 3. Protein-Protein interaction network of SMARCD3, CRIP2, PRAM1, HSPB2 and CERCAM.

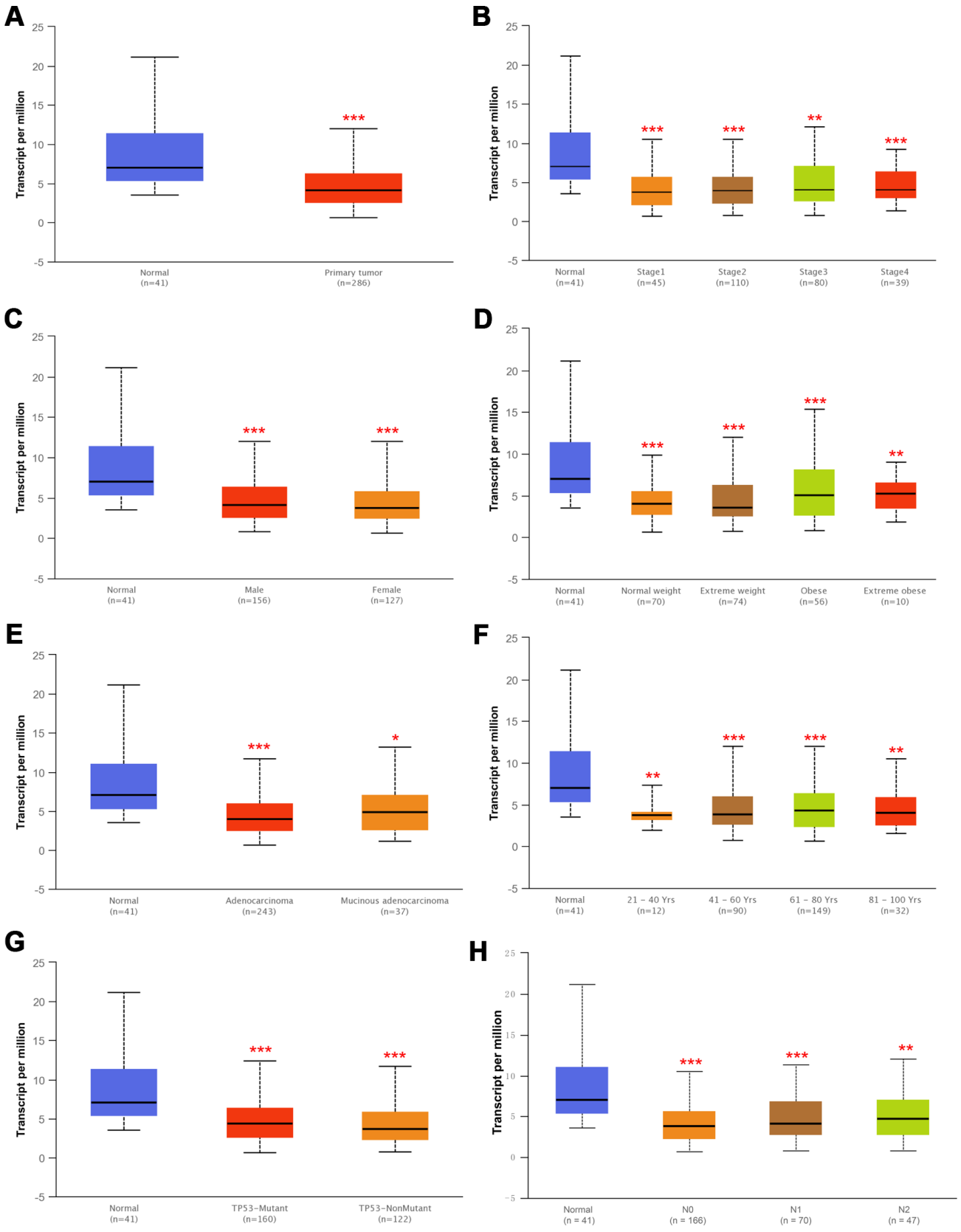

Supplementary Figure 4. SMARCD3 expression in different clinical subgroups. (**A**) SMARCD3 expression in colon cancer and normal controls. SMARCD3 expression in different cancer stage (**B**), gender (**C**), body weight (**D**), sample type (**E**), age (**F**), TP53 mutation status (**G**) and nodal metastasis status (**H**).

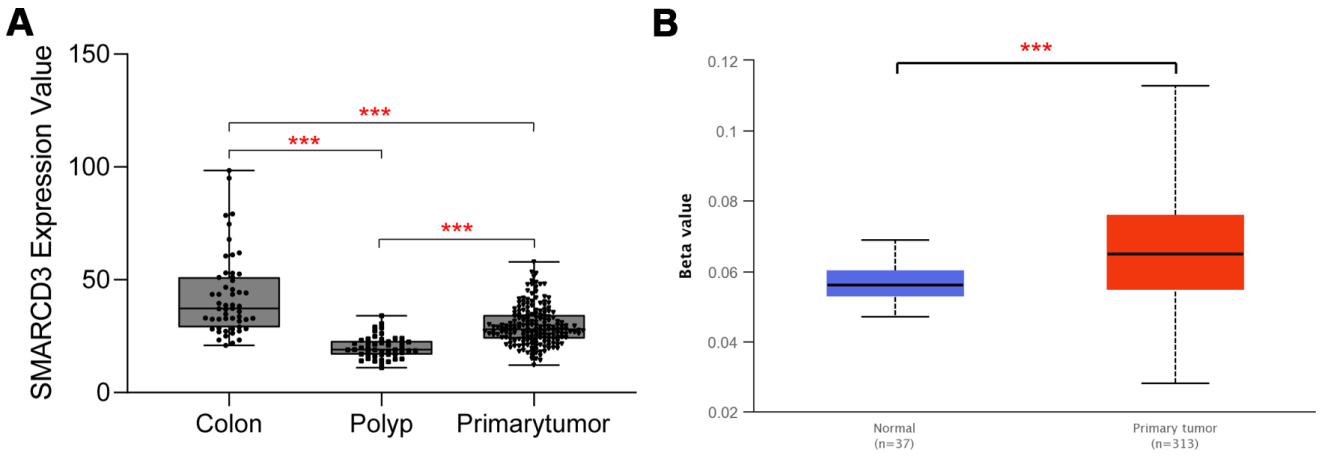

Supplementary Figure 5. (**A**) SMARCD3 expression in normal control, polyps and primary tumor. (**B**) the methylation level of SMARCD3 in primary tumor is significantly higher than normal control.

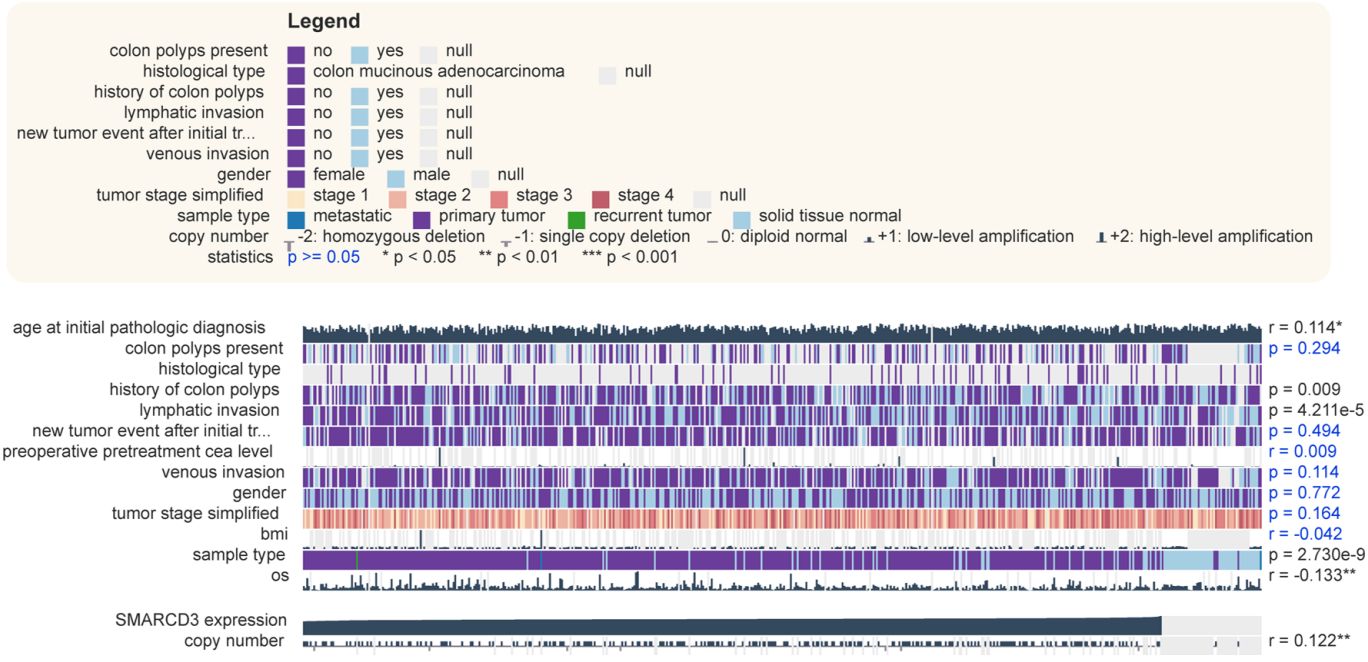

Supplementary Figure 6. Association between SMARCD3 expression levels and clinical features.

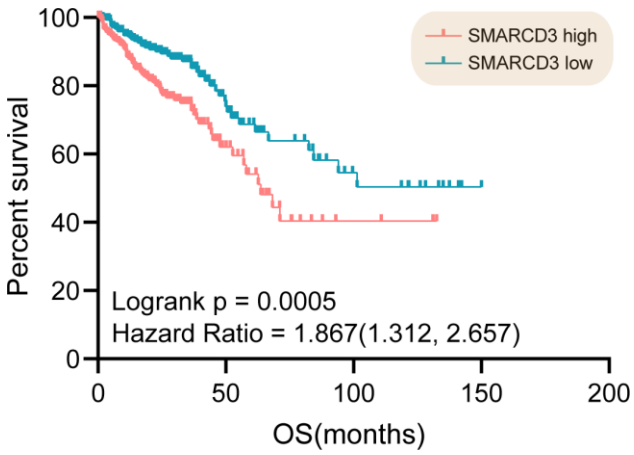

Supplementary Figure 7. Kaplan-Meier survival analysis based on SMARCD3 expression values using TCGA COAD RNAseq data (N = 592).

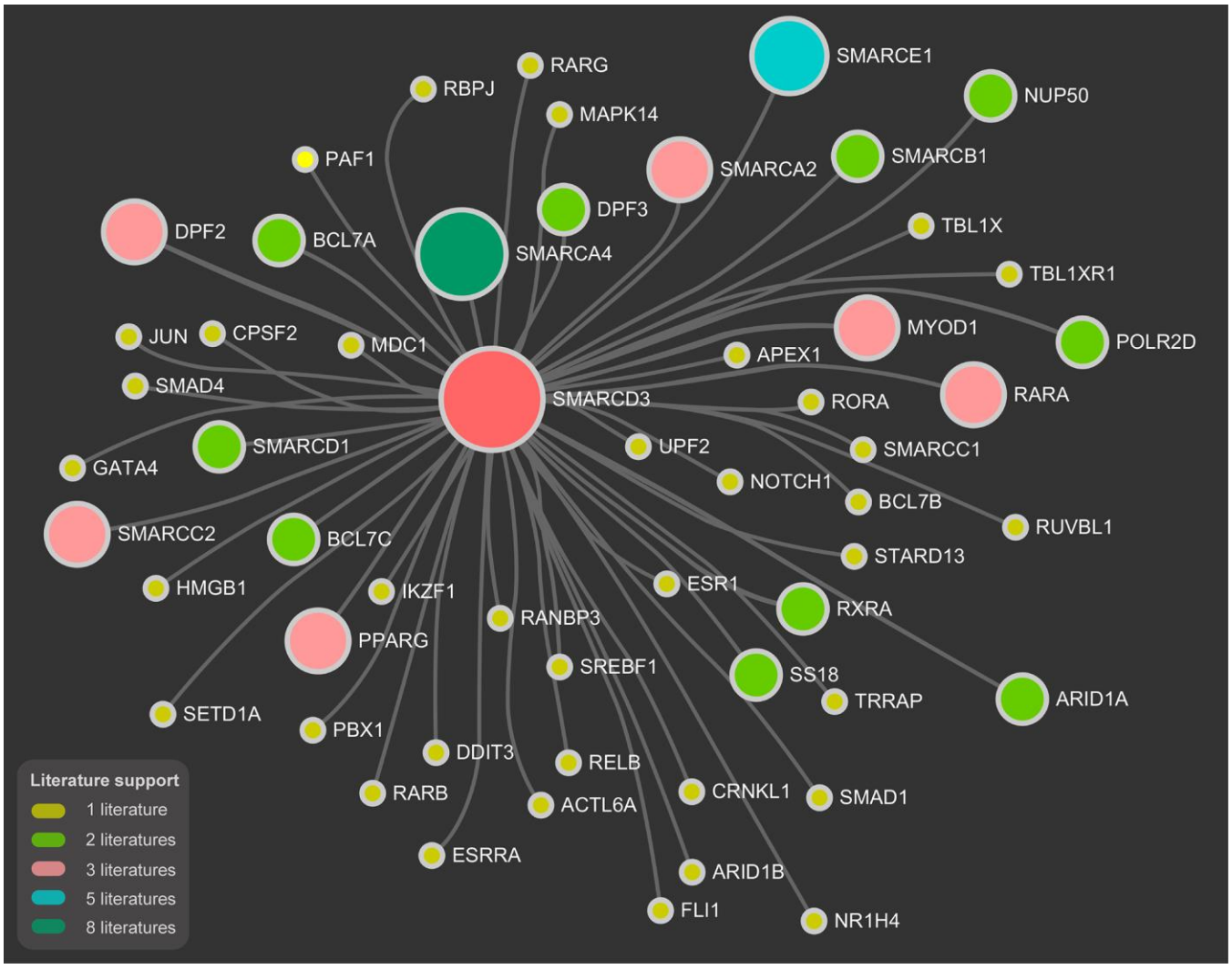

Supplementary Figure 8. Protein-Protein interaction network of SMARCD3 based on data from CTDbase.

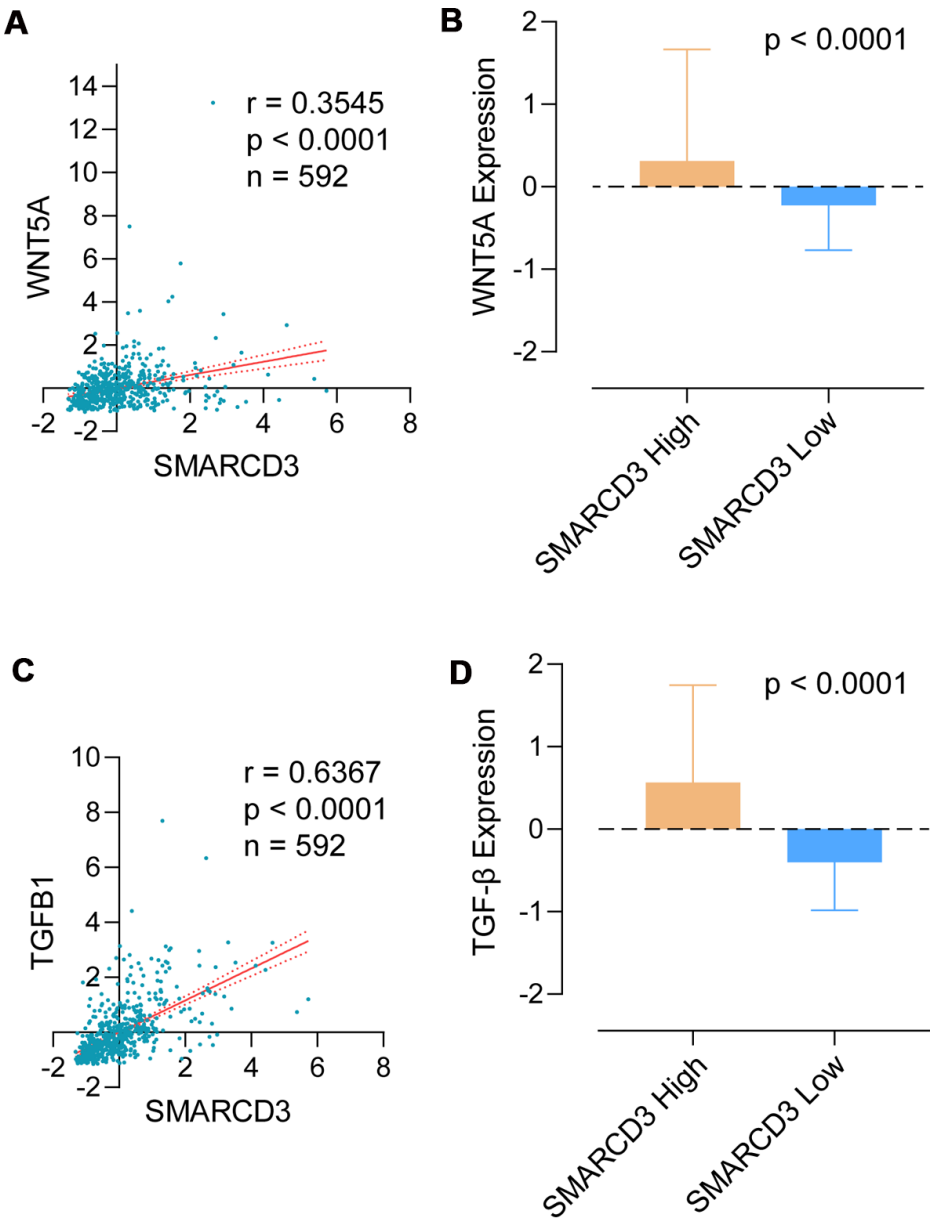

Supplementary Figure 9. SMARCD3 expression is positively correlated with WNT5A and TGF-β. (**A**) Correlation plot of WNT5A and SMARCD3. (**B**) WNT5A mRNA expression in SMARCD3 high and low groups. (**C**) Correlation plot of TGFB1 and SMARCD3. (**D**) TGFB1 mRNA expression in SMARCD3 high and low groups.

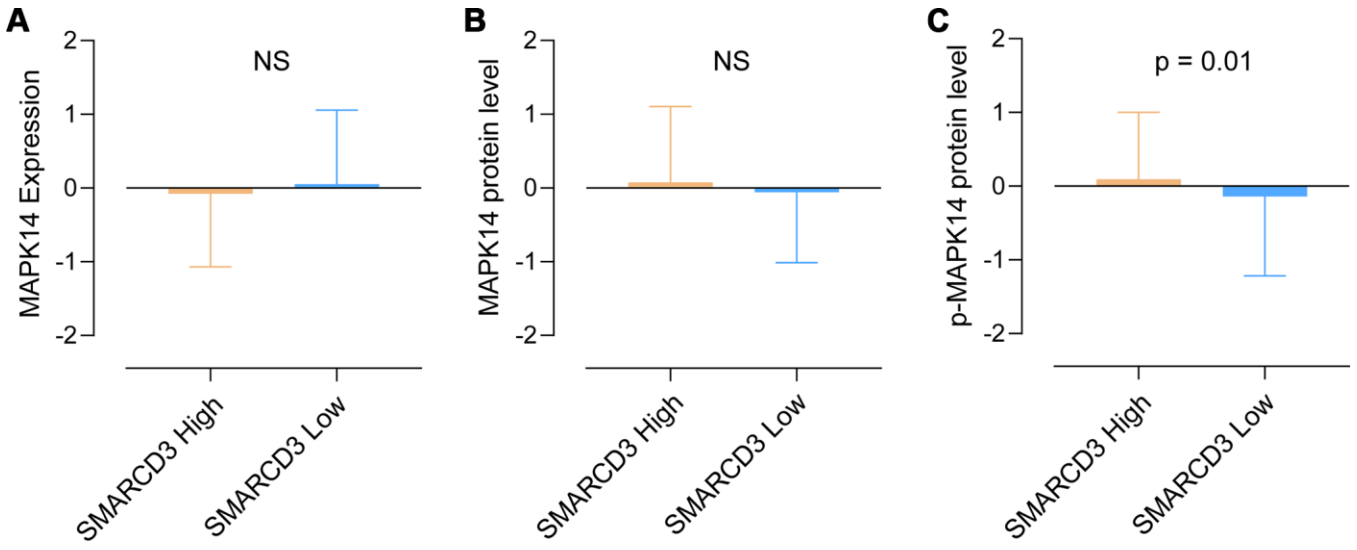

Supplementary Figure 10. SMARCD3 expression is positively correlated with MAPK14 phosphorylation levels. MAPK14 mRNA (**A**), MAPK14 protein (**B**) and p-MAPK14 protein (**C**) expression levels in SMARCD3 high and low groups.

Supplementary Tables

Please browse Full Text version to see the data of Supplementary Tables 1, 2, 6.

Supplementary Table 1. List of 372 commonly upregulated genes in TME.

Supplementary Table 2. GO analysis of 372 genes (Biological Process).

Supplementary Table 3. GO analysis of 372 genes (Cellular Component).

Pathway	Total	Expected	Hits	P.Value	FDR
Integral to plasma membrane	1270	26.3	79	2.82E-19	3.32E-17
External side of plasma membrane	204	4.22	32	2.95E-19	3.32E-17
Intrinsic to plasma membrane	1320	27.4	80	8.66E-19	6.49E-17
Plasma membrane part	2320	47.9	109	1.30E-17	7.30E-16
Cell surface	518	10.7	45	2.80E-16	1.26E-14
Plasma membrane	5500	114	185	1.28E-15	4.78E-14
Extracellular space	901	18.6	57	3.16E-14	1.02E-12
Extracellular region part	1320	27.3	71	5.00E-14	1.40E-12
Intrinsic to membrane	5760	119	182	2.11E-12	5.26E-11
Integral to membrane	5590	116	178	2.34E-12	5.26E-11
Lytic vacuole	401	8.3	29	5.34E-09	1.00E-07
Lysosome	401	8.3	29	5.34E-09	1.00E-07
Extracellular matrix	570	11.8	32	3.27E-07	5.53E-06
Vacuole	486	10.1	29	3.44E-07	5.53E-06
Extracellular region	2860	59.1	96	4.05E-07	6.08E-06
Membrane part	7520	156	201	5.16E-07	7.25E-06
Proteinaceous extracellular matrix	398	8.24	23	9.83E-06	0.00013
Collagen	93	1.92	10	2.23E-05	0.000279
Receptor complex	189	3.91	14	4.04E-05	0.000479
Vacuolar part	279	5.77	17	7.50E-05	0.000844
Extracellular matrix part	204	4.22	12	0.00115	0.012
Immunological synapse	23	0.476	4	0.00117	0.012
Lysosomal membrane	153	3.17	10	0.00133	0.013
Membrane raft	189	3.91	11	0.00198	0.0173
Ruffle	135	2.79	9	0.002	0.0173
Extrinsic to membrane	135	2.79	9	0.002	0.0173
Extrinsic to plasma membrane	87	1.8	7	0.00217	0.0181
Anchored to membrane	147	3.04	9	0.00355	0.0285
Actin filament	51	1.06	5	0.00397	0.0308
Integrin complex	32	0.662	4	0.0041	0.0308
Anchored to plasma membrane	33	0.683	4	0.00459	0.0333
Endocytic vesicle	187	3.87	10	0.00567	0.0398
Vacuolar membrane	206	4.26	10	0.0109	0.074
Vesicle	1210	25	34	0.0422	0.279
Membrane_bounded vesicle	1100	22.7	31	0.0493	0.317

Supplementary Table 4. GO analysis of 372 genes (Molecular Function).

Pathway	Total	Expected	Hits	P.Value	FDR
Receptor activity	1920	38.1	79	8.32E-11	3.23E-08
Carbohydrate binding	227	4.5	21	4.83E-09	6.25E-07
Carbohydrate binding	227	4.5	21	4.83E-09	6.25E-07
Cytokine activity	220	4.36	18	4.00E-07	3.88E-05
Glycosaminoglycan binding	178	3.53	15	2.61E-06	0.000203
Pattern recognition receptor activity	17	0.337	5	1.50E-05	0.000972
Cytokine receptor binding	266	5.27	17	2.32E-05	0.00124
Transmembrane signaling receptor activity	1510	30	53	2.56E-05	0.00124
Cytokine receptor activity	106	2.1	10	4.76E-05	0.00185
Cytokine receptor activity	106	2.1	10	4.76E-05	0.00185
Chemokine activity	50	0.991	7	5.38E-05	0.0019
Chemokine receptor binding	75	1.49	8	0.000115	0.00373
Cytokine binding	66	1.31	7	0.00032	0.00887
Cytokine binding	66	1.31	7	0.00032	0.00887
Protein complex binding	339	6.72	17	0.000441	0.0114
Receptor binding	1590	31.6	49	0.00118	0.0286
Lipoprotein particle binding	26	0.515	4	0.0016	0.0365
Antigen binding	66	1.31	6	0.00193	0.0412
Lipid binding	788	15.6	28	0.00202	0.0412
Collagen binding	47	0.931	5	0.00229	0.0445
Enzyme activator activity	436	8.64	18	0.00275	0.0508
Low_density lipoprotein particle binding	15	0.297	3	0.00294	0.0518
Phospholipid binding	514	10.2	19	0.00694	0.117
Metalloexopeptidase activity	42	0.832	4	0.00936	0.151
Peptide receptor activity	150	2.97	8	0.0101	0.157
Non_membrane spanning protein tyrosine kinase activity	46	0.912	4	0.0128	0.192
Identical protein binding	910	18	28	0.0138	0.198
Heparin binding	130	2.58	7	0.0149	0.207
GTP binding	371	7.35	14	0.0163	0.214
Antioxidant activity	75	1.49	5	0.0165	0.214
G_protein coupled receptor binding	232	4.6	10	0.0175	0.219
Protein homodimerization activity	573	11.4	19	0.02	0.243
Extracellular matrix structural constituent	80	1.59	5	0.0213	0.25
Kinase regulator activity	144	2.85	7	0.0247	0.282
Guanyl nucleotide binding	402	7.97	14	0.0298	0.33
Growth factor binding	125	2.48	6	0.0382	0.407
Protein dimerization activity	996	19.7	28	0.0388	0.407
Phosphatidylinositol binding	160	3.17	7	0.0403	0.411
Rho GTPase activator activity	39	0.773	3	0.0417	0.415
Phospholipase C activity	41	0.813	3	0.0473	0.458

Supplementary Table 5. KEGG pathway analysis of 372 genes.

Pathway	Total	Expected	Hits	P.Value	FDR
Osteoclast differentiation	128	3.23	31	1.52E-22	4.85E-20
Staphylococcus aureus infection	68	1.71	18	3.24E-14	5.16E-12
Tuberculosis	179	4.51	22	5.63E-10	5.97E-08
Leishmaniasis	74	1.87	14	3.17E-09	2.52E-07
Toll-like receptor signaling pathway	104	2.62	16	5.43E-09	3.32E-07
Rheumatoid arthritis	91	2.29	15	6.27E-09	3.32E-07
Hematopoietic cell lineage	97	2.44	15	1.55E-08	7.03E-07
Cytokine-cytokine receptor interaction	294	7.41	25	7.67E-08	3.05E-06
Chemokine signaling pathway	190	4.79	19	2.61E-07	9.21E-06
Pertussis	76	1.92	12	3.54E-07	1.13E-05
Chagas disease (American trypanosomiasis)	103	2.6	13	1.63E-06	4.70E-05
Malaria	49	1.23	9	2.93E-06	7.77E-05
Complement and coagulation cascades	79	1.99	11	3.98E-06	9.73E-05
Phagosome	152	3.83	15	5.92E-06	0.000135
Leukocyte transendothelial migration	112	2.82	12	2.28E-05	0.000483
Lysosome	123	3.1	12	5.82E-05	0.00116
Cell adhesion molecules (CAMs)	146	3.68	13	7.45E-05	0.00139
Intestinal immune network for IgA production	49	1.23	7	0.000203	0.00359
B cell receptor signaling pathway	71	1.79	8	0.000385	0.00645
Legionellosis	55	1.39	7	0.000422	0.00672
NOD-like receptor signaling pathway	178	4.49	13	0.000536	0.00811
NF-kappa B signaling pathway	100	2.52	9	0.000897	0.013
Influenza A	167	4.21	12	0.00101	0.014
Inflammatory bowel disease (IBD)	65	1.64	7	0.00117	0.0155
Natural killer cell mediated cytotoxicity	131	3.3	10	0.00168	0.0214
TNF signaling pathway	110	2.77	9	0.00176	0.0216
Systemic lupus erythematosus	133	3.35	10	0.00188	0.0222
Fc gamma R-mediated phagocytosis	91	2.29	8	0.002	0.0228
Toxoplasmosis	113	2.85	9	0.00213	0.0233
Measles	138	3.48	10	0.00248	0.0251
Kaposi's sarcoma-associated herpesvirus infection	186	4.69	12	0.00253	0.0251
Transcriptional misregulation in cancer	186	4.69	12	0.00253	0.0251
T cell receptor signaling pathway	101	2.55	8	0.00385	0.0371
Proteoglycans in cancer	201	5.07	12	0.00475	0.0445
Th17 cell differentiation	107	2.7	8	0.00547	0.0497
Acute myeloid leukemia	66	1.66	6	0.00615	0.0543
Th1 and Th2 cell differentiation	92	2.32	7	0.00835	0.0699
Fluid shear stress and atherosclerosis	139	3.5	9	0.00835	0.0699
Amoebiasis	96	2.42	7	0.0105	0.0852
Prion diseases	35	0.882	4	0.0111	0.0884
Antigen processing and presentation	77	1.94	6	0.0128	0.0978
AGE-RAGE signaling pathway in diabetic complications	100	2.52	7	0.0129	0.0978
Allograft rejection	38	0.958	4	0.0148	0.109
Graft-versus-host disease	41	1.03	4	0.0191	0.138

Jak-STAT signaling pathway	162	4.08	9	0.0211	0.149
Fc epsilon RI signaling pathway	68	1.71	5	0.028	0.194
IL-17 signaling pathway	93	2.34	6	0.0296	0.198
Sphingolipid signaling pathway	119	3	7	0.0304	0.198
Epstein-Barr virus infection	201	5.07	10	0.0305	0.198
RIG-I-like receptor signaling pathway	70	1.76	5	0.0312	0.199
PI3K-Akt signaling pathway	354	8.92	15	0.0335	0.209
Platelet activation	124	3.13	7	0.0369	0.225
Asthma	31	0.781	3	0.0422	0.253
Pathogenic Escherichia coli infection	55	1.39	4	0.0493	0.289
HTLV-I infection	219	5.52	10	0.0499	0.289

Supplementary Table 6. COAD specific Protein-Protein network analysis of 372 genes.

Supplementary Table 7. Pearson correlation of SMARCD3 expression with different cell types in TME.

Cell type	Spearman r	95% confidence interval	P (two-tailed)	P value summary	Exact or approximate P value?	Significant? (alpha = 0.05)
Fibroblasts	0.6773	0.6158 to 0.7306	<0.0001	****	Approximate	Yes
Chondrocytes	0.6335	0.5658 to 0.6927	<0.0001	****	Approximate	Yes
Astrocytes	0.6248	0.5559 to 0.6851	<0.0001	****	Approximate	Yes
HSC	0.52	0.4385 to 0.5930	<0.0001	****	Approximate	Yes
Mesangial cells	0.4945	0.4104 to 0.5702	<0.0001	****	Approximate	Yes
Endothelial cells	0.472	0.3857 to 0.5501	<0.0001	****	Approximate	Yes
Pericytes	0.4678	0.3811 to 0.5463	<0.0001	****	Approximate	Yes
ly Endothelial cells	0.4661	0.3793 to 0.5448	<0.0001	****	Approximate	Yes
Macrophages M1	0.4653	0.3783 to 0.5441	<0.0001	****	Approximate	Yes
mv Endothelial cells	0.4469	0.3583 to 0.5275	<0.0001	****	Approximate	Yes
Adipocytes	0.4385	0.3492 to 0.5200	<0.0001	****	Approximate	Yes
Macrophages	0.4171	0.3259 to 0.5006	<0.0001	****	Approximate	Yes
aDC	0.4127	0.3211 to 0.4966	<0.0001	****	Approximate	Yes
DC	0.3992	0.3066 to 0.4843	<0.0001	****	Approximate	Yes
MSC	0.3889	0.2956 to 0.4750	<0.0001	****	Approximate	Yes
CD4+ naive T-cells	0.331	0.2336 to 0.4218	<0.0001	****	Approximate	Yes
Melanocytes	0.2645	0.1635 to 0.3600	<0.0001	****	Approximate	Yes
Monocytes	0.2571	0.1558 to 0.3531	<0.0001	****	Approximate	Yes
Megakaryocytes	0.2538	0.1524 to 0.3499	<0.0001	****	Approximate	Yes
iDC	0.23	0.1276 to 0.3276	<0.0001	****	Approximate	Yes
Neurons	0.2055	0.1022 to 0.3044	<0.0001	****	Approximate	Yes
cDC	0.1788	0.07472 to 0.2791	0.0006	***	Approximate	Yes
Eosinophils	0.1776	0.07346 to 0.2779	0.0006	***	Approximate	Yes
Myocytes	0.162	0.05742 to 0.2630	0.0019	**	Approximate	Yes
GMP	0.1603	0.05569 to 0.2614	0.0021	**	Approximate	Yes
Neutrophils	0.1258	0.02056 to 0.2283	0.016	*	Approximate	Yes
CD8+ Tem	0.1173	0.01194 to 0.2201	0.0248	*	Approximate	Yes
Hepatocytes	0.07119	-0.03459 to 0.1754	0.1741	ns	Approximate	No
Skeletal muscle	0.06895	-0.03684 to 0.1732	0.1881	ns	Approximate	No
CMP	0.06416	-0.04164 to 0.1685	0.2208	ns	Approximate	No
CD4+ Tcm	0.052	-0.05381 to 0.1567	0.3212	ns	Approximate	No
CD8+ Tcm	0.04653	-0.05928 to 0.1513	0.3748	ns	Approximate	No
CD8+ T-cells	0.0126	-0.09304 to 0.1180	0.8102	ns	Approximate	No
Tregs	0.00172	-0.1038 to 0.1072	0.9738	ns	Approximate	No
CD4+ T-cells	-0.008136	-0.1136 to 0.09747	0.8767	ns	Approximate	No
Mast cells	-0.01023	-0.1156 to 0.09539	0.8454	ns	Approximate	No
Class-switched memory B-cells	-0.04365	-0.1485 to 0.06215	0.405	ns	Approximate	No
Tgd cells	-0.05474	-0.1593 to 0.05107	0.2963	ns	Approximate	No
MPP	-0.06603	-0.1704 to 0.03976	0.2075	ns	Approximate	No
B-cells	-0.0714	-0.1756 to 0.03438	0.1729	ns	Approximate	No
NK cells	-0.07455	-0.1787 to 0.03121	0.1546	ns	Approximate	No
Platelets	-0.09096	-0.1946 to 0.01469	0.0822	ns	Approximate	No
Sebocytes	-0.09207	-0.1957 to 0.01358	0.0786	ns	Approximate	No

CD8+ naive T-cells	-0.09239	-0.1960 to 0.01326	0.0775	ns	Approximate	No
Erythrocytes	-0.123	-0.2256 to -0.01773	0.0185	*	Approximate	Yes
Macrophages M2	-0.1236	-0.2262 to -0.01834	0.018	*	Approximate	Yes
pDC	-0.1642	-0.2652 to -0.05975	0.0016	**	Approximate	Yes
CD4+ Tem	-0.1811	-0.2812 to -0.07703	0.0005	***	Approximate	Yes
Preadipocytes	-0.1983	-0.2976 to -0.09473	0.0001	***	Approximate	Yes
CD4+ memory T-cells	-0.2133	-0.3118 to -0.1103	<0.0001	****	Approximate	Yes
Epithelial cells	-0.2158	-0.3142 to -0.1129	<0.0001	****	Approximate	Yes
Basophils	-0.2161	-0.3145 to -0.1132	<0.0001	****	Approximate	Yes
Memory B-cells	-0.2192	-0.3173 to -0.1163	<0.0001	****	Approximate	Yes
naive B-cells	-0.2487	-0.3452 to -0.1471	<0.0001	****	Approximate	Yes
Smooth muscle	-0.253	-0.3492 to -0.1515	<0.0001	****	Approximate	Yes
Keratinocytes	-0.2623	-0.3579 to -0.1612	<0.0001	****	Approximate	Yes
Th2 cells	-0.2733	-0.3682 to -0.1727	<0.0001	****	Approximate	Yes
CLP	-0.2904	-0.3842 to -0.1907	<0.0001	****	Approximate	Yes
pro B-cells	-0.3101	-0.4025 to -0.2115	<0.0001	****	Approximate	Yes
MEP	-0.3131	-0.4052 to -0.2146	<0.0001	****	Approximate	Yes
NKT	-0.3256	-0.4168 to -0.2279	<0.0001	****	Approximate	Yes
Osteoblast	-0.3262	-0.4174 to -0.2286	<0.0001	****	Approximate	Yes
Plasma cells	-0.3272	-0.4183 to -0.2296	<0.0001	****	Approximate	Yes
Th1 cells	-0.3425	-0.4324 to -0.2459	<0.0001	****	Approximate	Yes

Supplementary Table 8. KEGG pathway analysis of SMARCD3 Protein-Protein network.

Pathway	Total	Expected	Hits	P.Value	FDR
Transcriptional misregulation in cancer	186	0.769	8	6.16E-07	0.000196
Th17 cell differentiation	107	0.443	6	4.11E-06	0.000654
Wnt signaling pathway	158	0.653	5	0.00043	0.0415
Th1 and Th2 cell differentiation	92	0.381	4	0.000522	0.0415
Endocrine resistance	98	0.405	4	0.000663	0.0422
Pathways in cancer	530	2.19	8	0.00111	0.0567
Thyroid hormone signaling pathway	116	0.48	4	0.00125	0.0567
Osteoclast differentiation	128	0.529	4	0.0018	0.0662
HTLV-I infection	219	0.906	5	0.00187	0.0662
Non-alcoholic fatty liver disease (NAFLD)	149	0.616	4	0.00312	0.0993
AGE-RAGE signaling pathway in diabetic complications	100	0.414	3	0.00792	0.229
Epstein-Barr virus infection	201	0.831	4	0.00899	0.238
Thyroid cancer	37	0.153	2	0.0101	0.247
Notch signaling pathway	48	0.199	2	0.0166	0.377
Estrogen signaling pathway	138	0.571	3	0.0189	0.382
Signaling pathways regulating pluripotency of stem cells	139	0.575	3	0.0192	0.382
Breast cancer	147	0.608	3	0.0223	0.417
Hepatitis B	163	0.674	3	0.0291	0.455
Inflammatory bowel disease (IBD)	65	0.269	2	0.0293	0.455
Non-small cell lung cancer	66	0.273	2	0.0302	0.455
Epithelial cell signaling in Helicobacter pylori infection	68	0.281	2	0.0319	0.455
MAPK signaling pathway	295	1.22	4	0.0321	0.455
Prolactin signaling pathway	70	0.29	2	0.0336	0.455
Bile secretion	72	0.298	2	0.0354	0.455
PPAR signaling pathway	74	0.306	2	0.0372	0.455
Leishmaniasis	74	0.306	2	0.0372	0.455
Pertussis	76	0.314	2	0.0391	0.46
Salmonella infection	86	0.356	2	0.0488	0.525
Colorectal cancer	86	0.356	2	0.0488	0.525